L1CAM/Neuroglian controls the axon–axon interactions establishing layered and lobular mushroom body architecture

Dominique Siegenthaler,[1,2] Eva-Maria Enneking,[1,2] Eliza Moreno,[1] and Jan Pielage[1]

[1]Friedrich Miescher Institute for Biomedical Research, 4058 Basel, Switzerland
[2]University of Basel, 4003 Basel, Switzerland

The establishment of neuronal circuits depends on the guidance of axons both along and in between axonal populations of different identity; however, the molecular principles controlling axon–axon interactions in vivo remain largely elusive. We demonstrate that the *Drosophila melanogaster* L1CAM homologue Neuroglian mediates adhesion between functionally distinct mushroom body axon populations to enforce and control appropriate projections into distinct axonal layers and lobes essential for olfactory learning and memory. We addressed the regulatory mechanisms controlling homophilic Neuroglian-mediated cell adhesion by analyzing targeted mutations of extra- and intracellular Neuroglian domains in combination with cell type–specific rescue assays in vivo. We demonstrate independent and cooperative domain requirements: intercalating growth depends on homophilic adhesion mediated by extracellular Ig domains. For functional cluster formation, intracellular Ankyrin2 association is sufficient on one side of the trans-axonal complex whereas Moesin association is likely required simultaneously in both interacting axonal populations. Together, our results provide novel mechanistic insights into cell adhesion molecule–mediated axon–axon interactions that enable precise assembly of complex neuronal circuits.

Introduction

The ability of the brain to process and store information requires the assembly of neurons into complex circuits. This process depends on appropriate guidance of axons to distant targets. Although significant progress has been made regarding the identification of signaling systems controlling long-range axon guidance (Kolodkin and Tessier-Lavigne, 2011), the molecular and cellular mechanisms controlling axon–axon interactions between neuronal populations at guidance choice points in vivo remain largely unknown. To address the molecular mechanisms controlling the establishment of complex axonal assemblies, we used the *Drosophila* mushroom bodies (MBs), a bilaterally symmetric central brain structure essential for olfactory learning and memory, as a model system (de Belle and Heisenberg, 1994). The MBs are composed of ∼2,000 Kenyon cells (KCs; Heisenberg, 2003) derived from four neuroblasts (NBs) that in a sequential manner give rise to three genetically, anatomically, and functionally distinct subpopulations (γ, α′β′, and αβ neurons; Crittenden et al., 1998; Lee et al., 1999; Krashes et al., 2007; Trannoy et al., 2011). During embryonic and early larval development, axons of γ neurons fasciculate into a single bundle below the MB calyx and project via the pedunculus, the major axonal MB tract, to the anterior brain, where they branch into medial and vertical lobes. During late larval stages, α′β′ axons are born (Lee and Luo, 1999) that form a subtype-specific fascicle and intercalate at the center of the pedunculus in between γ axons (Kurusu et al., 2002). At the end of the pedunculus (pedunculus divide), the axons branch to form medial and vertical lobes in close proximity to γ lobes. Finally, at early pupal stages, axons of αβ neurons intercalate in between α′β′ neurons, thereby forming a third concentric axonal layer within the pedunculus (Kurusu et al., 2002) and vertical and medial lobes next to α′β′ lobes in the anterior brain (Fig. 1 A). Thus, MB axons of different identity form highly associated but strictly segregated axonal layers and lobes. The importance of the anatomical segregation is reflected

Correspondence to Jan Pielage: jan.pielage@fmi.ch

Abbreviations used in this paper: Ank2, Ankyrin2; CAM, cell adhesion molecule; Dlg, Discs large; FasII, Fasciclin II; MARCM, mosaic analysis with a repressible cell marker; MB, mushroom body; NB, neuroblast; Nrg, Neuroglian.

The Rockefeller University Press $30.00
J. Cell Biol. Vol. 208 No. 7 1003–1018
www.jcb.org/cgi/doi/10.1083/jcb.201407131

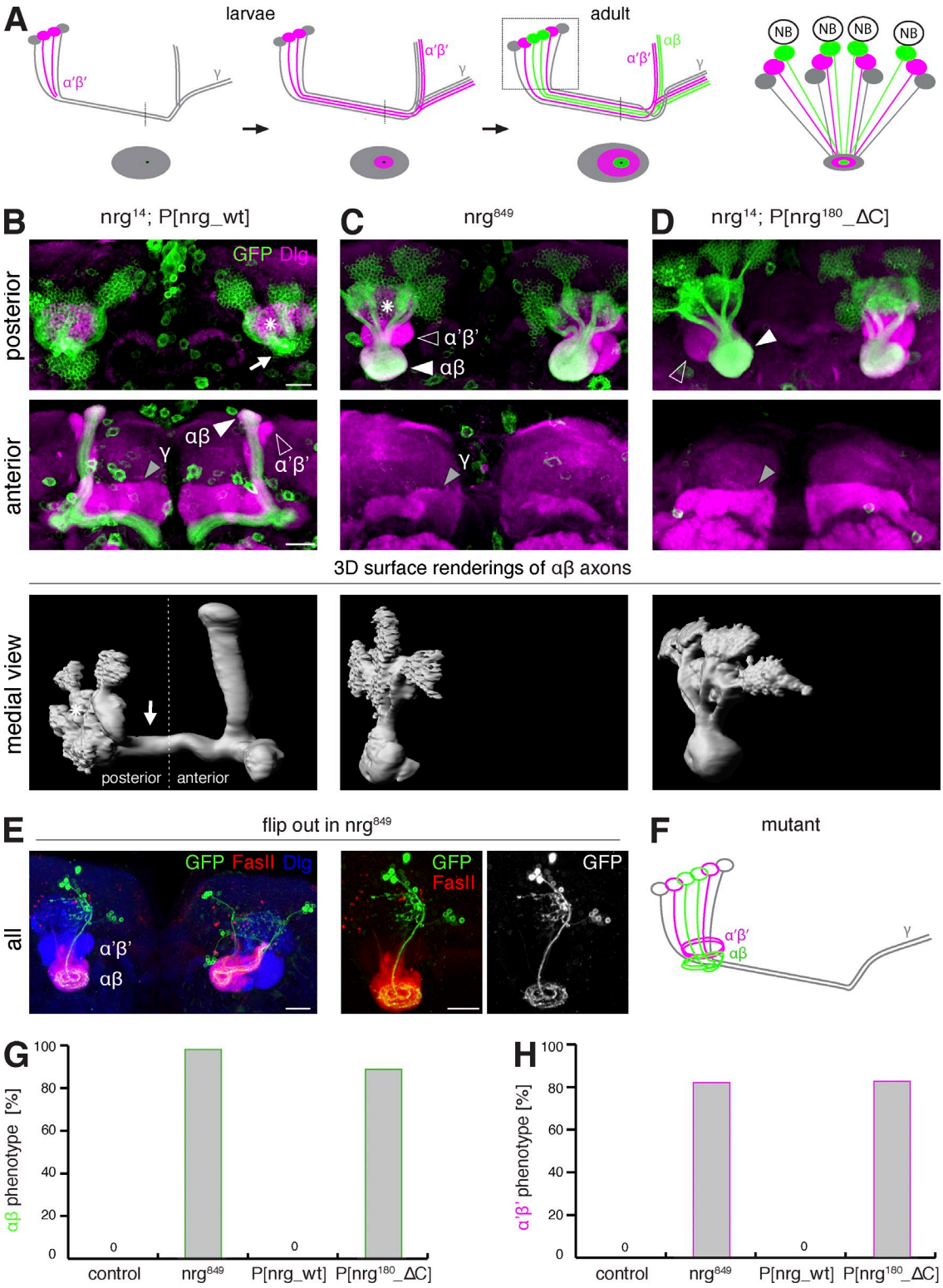

Figure 1. **Extra- and intracellular Nrg domains contribute to MB axon guidance.** (A) Schematic drawings of MB development. Side views of MB axon projections and cross-sections of the pedunculus are shown: γ (gray), α'β' (magenta), and αβ (green). (B–D) Frontal projections of posterior (top) and anterior (middle) regions of the MBs. αβ neurons are marked by mCD8-GFP expression (*c739*-Gal4, green), and neurites of all MB are visualized by Dlg (magenta). Bottom panels show medial (side) views of 3D-surface rendered αβ neurons. (B) In *nrg*^{14}*;* P[*nrg_wt*] control animals, axons of all three MB neuron subtypes project through the pedunculus (arrows) into vertical and medial MB lobes (arrowheads). (C and D) In *nrg* mutant animals carrying either a mutation in the extracellular domain (B; *nrg*^{849}) or lacking the Nrg^{180}-specific C terminus (C; *nrg*^{14}*;* P[*nrg*^{180}*_ΔC*]), axons of αβ (green) and α'β' (magenta/white) neurons fail to project into the pedunculus and accumulate in ball-like structures in the posterior brain ventral to the calyx (asterisks). αβ and α'β' axons remain segregated (top, arrowheads). Axons of γ neurons (middle, arrowheads) still form a medial lobe that is often thinner compared with controls. (E) Frontal projections of entire MBs of an *nrg*^{849} mutant in which individual αβ neurons are labeled by mCD8-GFP (*201Y*-Gal4) using a flip-out approach. αβ axons are marked with FasII (red), neuropil with Dlg (blue). Bars, 20 µm. (F) Schematic model of axonal projections in *nrg*^{14}*;* P[*nrg*^{180}*_ΔC*] mutant animals.

by the functional disparity and unique requirements of γ, α′β′, and αβ neurons for olfactory memory acquisition, storage, and retrieval (Krashes et al., 2007; Blum et al., 2009; Trannoy et al., 2011; Qin et al., 2012). Similarly, during establishment of complex neuronal circuitry in vertebrates, axons of different identity and function are known to interact (Gallarda et al., 2008; Chen et al., 2012; Nishikimi et al., 2013; Schmidt et al., 2014), but the underlying molecular mechanisms remain largely unknown. Cell adhesion molecules (CAMs) represent likely candidates to establish and regulate the cell–cell contacts necessary to control axonal intercalation.

To address these questions, we focused on the Ig-family CAM Neuroglian (Nrg), which has been shown to be essential for MB development (Strauss and Heisenberg, 1993; Carhan et al., 2005; Goossens et al., 2011). Nrg encodes the *Drosophila* orthologue of the L1CAM family and shares a similar homology to all four vertebrate protein family members (L1, CHL1, NrCAM, and Neurofascin; Bieber et al., 1989). L1 family members represent single-pass transmembrane proteins and can mediate cellular adhesion by forming homo- or heterophilic interactions with their extracellular domain (Hortsch, 2000; Maness and Schachner, 2007; Sakurai, 2012). The cytoplasmic tail of vertebrate L1-type family members and Nrg consist of 85–145 aa (Hortsch, 2000) harboring highly conserved protein–protein interacting domains mediating binding to cytoskeletal adaptor proteins including Ankyrins (Davis and Bennett, 1994; Dubreuil et al., 1996) and Ezrin-Radizin-Moesin (ERM) proteins (Dickson et al., 2002). It has been demonstrated that these intracellular interactions contribute to L1-dependent axonal outgrowth of cultured neurons by establishing static cell–cell interactions (Ankyrins; Gil et al., 2003) or traction force generation (Ezrin; Sakurai et al., 2008). In *Drosophila* it has been shown that Nrg contributes to axon guidance of peripheral neurons (Hall and Bieber, 1997; García-Alonso et al., 2000) and is essential for synapse maturation and maintenance (Enneking et al., 2013). The general importance of L1CAM for nervous system development is further underscored by the severe neurological phenotypes of human patients harboring mutations in L1. Extra- and intracellular mutations can result in hypoplasia of the corpus callosum and mental retardation, and are often accompanied by additional developmental defects summarized as L1 syndrome (Fransen et al., 1995, 1998; Yamasaki et al., 1997; Kamiguchi et al., 1998).

Here we systematically combine targeted domain-specific mutations with cell type–specific rescues to identify the molecular requirements of Nrg for axon–axon interactions and to gain insights into the cellular mechanisms controlling establishment of the complex MB architecture.

Results

Extra- and intracellular domains of Nrg are essential for MB axon guidance

To gain insights into the cellular and molecular mechanisms controlling formation of the complex axonal architecture of the *Drosophila* MBs (Fig. 1 A), we focused on the CAM Nrg, the *Drosophila* L1CAM homologue. Although it has been shown that extracellular Nrg-mediated adhesion is required for MB development (Goossens et al., 2011), the precise cellular and molecular requirements have not been addressed. To address these questions and to identify potential regulatory mechanisms, we first compared mutations affecting extracellular adhesion, nrg^{849} (Goossens et al., 2011), with mutations disrupting intracellular protein–protein interactions. To generate specific intracellular mutations, we used a genomic rescue approach (Venken et al., 2009) that allows expression of modified versions of Nrg at endogenous levels in the background of the embryonic-lethal nrg^{14} null mutation (Enneking et al., 2013). Importantly, in nrg^{14}-null mutant flies rescued by a wild-type Pacman construct (nrg^{14}; P[*nrg_wt*]), all MB axons project through the pedunculus (Fig. 1 B, arrow) to the anterior part of the brain, where they branch and project into vertical and medial lobes indistinguishable from controls (Fig. 1, B, G, and H). In contrast, in nrg^{849} mutants and *nrg* mutants lacking the Nrg^{180}-specific intracellular tail (nrg^{14}; P[nrg^{180}*_ΔC*]; see Fig. 4 H), both α′β′ and αβ axons fail to project into the pedunculus despite the presence of γ lobes (Fig. 1, C–H). Strikingly, α′β′ and αβ axons remained segregated and formed two separate ball-like structures ventral to the MB calyx (Fig. 1, C and D). These data demonstrate that protein–protein interactions mediated by the cytoplasmic tail domain of Nrg^{180} are essential for MB development, indicating that intracellular interactions directly contribute to functional properties of Nrg in vivo despite being dispensable for homophilic adhesion in cellular assays (Hortsch et al., 1995). The nrg^{849} mutant phenotype has previously been described as axon stalling (Goossens et al., 2011). However, based on the close phenotypic resemblance with mutations in the *rac* family of actin regulators that are due to defects in MB axon guidance (Ng et al., 2002), we next analyzed the projection patterns of individual axons. We labeled individual αβ axons in nrg^{849} mutants using a flip-out approach (Gordon and Scott, 2009). GFP-labeled mutant αβ axons projected through the area of aberrant α′β′ axons (Discs large [Dlg] positive, Fasciclin II [FasII] negative) into the ball-like αβ structure (FasII positive) but failed to grow anteriorly (Fig. 1 E). Instead, the axons grew in circles without leaving the aberrant FasII-positive area (Fig. 1 E). Thus, the observed phenotypes likely represent a failure of *nrg* mutant axons to enter the pedunculus and are consistent with an axon guidance but not with an axon stalling phenotype (Fig. 1 F).

We next addressed whether the observed αβ and α′β′ projection phenotypes were potentially due to failed lobular innervation of γ neurons during larval development, which precedes αβ and α′β′ development (Fig. 1 A and Fig. S1, A–C). In contrast to a prior report (Goossens et al., 2011), we observed severe axon projection defects of α′β′ neurons resulting in posterior ball-like structures in both the extra- and intracellular *nrg* mutations at the third instar larval stage (Fig. S1, D–F and G).

(G and H) Quantification of aberrant ball-like projections of αβ (G) or α′β′ (H) neurons. Phenotypes were assayed using FasII (αβ) or Trio (α′β′). *n* = 60, 46, 44, and 54 (G) and *n* = 26, 28, 24, and 34 (H), in the respective order of the genotypes indicated.

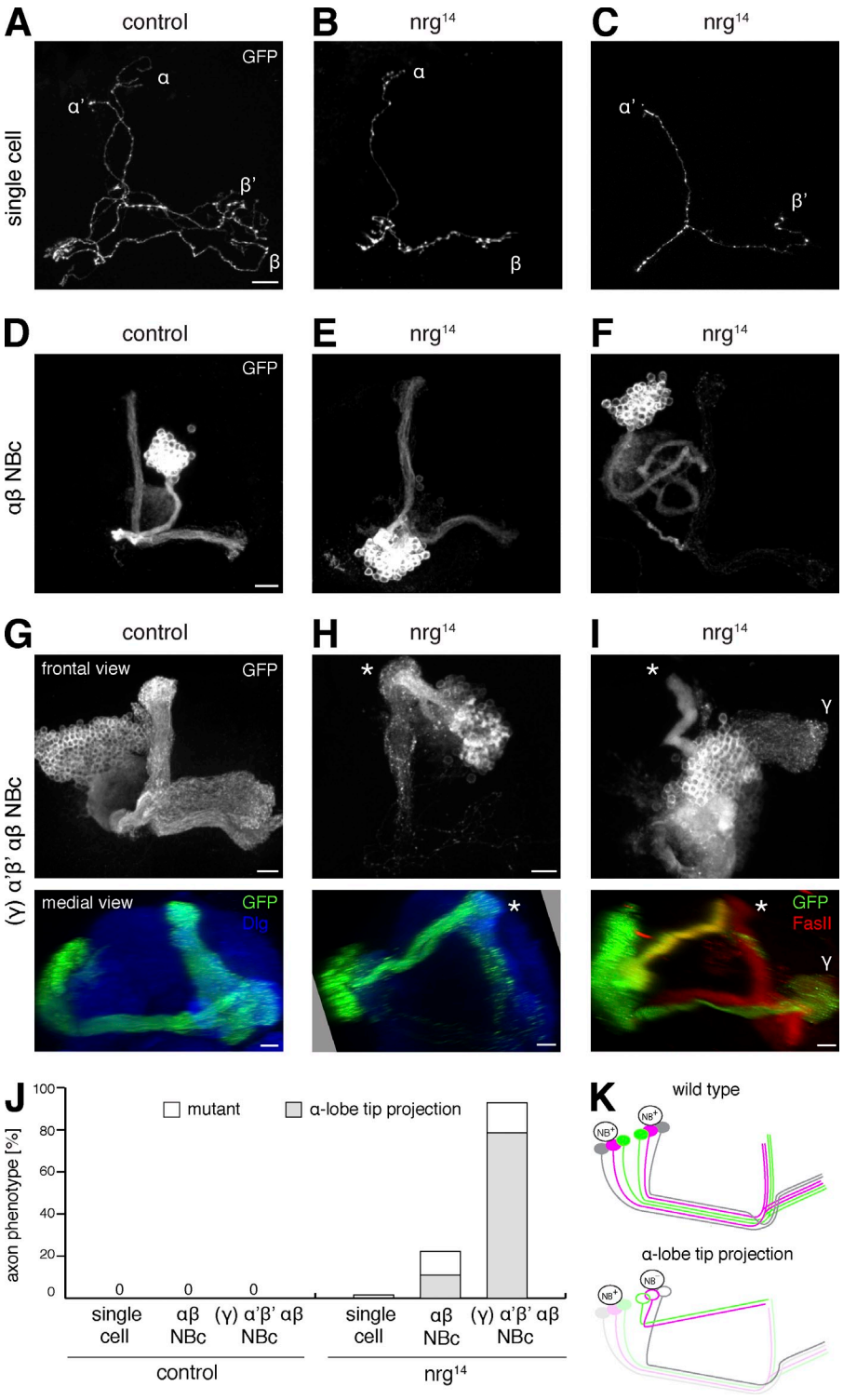

Figure 2. **Nrg controls MB axon tract choice.** (A–I) MARCM analysis of *nrg*^{14} mutants. Bars, 10 µm. (A–C) Frontal projections of control and *nrg*^{14} mutant single-cell clones. Absence of *nrg*^{14} in individual MB neurons does not cause obvious alteration of axonal projections. (D–F) Frontal projections of control and *nrg*^{14} αβ NB clones (NBc). The majority of *nrg*^{14} αβ NBc do not show an axonal phenotype (E). (F) Example of an *nrg*^{14} αβ NBc in which axons fail to project into the pedunculus and form circular projections in the posterior brain. (G–I) Large control and *nrg*^{14} NBc that include either α'β' and αβ (H) or all three MB subtypes (G and I). Top panels show frontal projections of the entire MB. Bottom panels show medial (side) views of the NBc marked by GFP (green) and Dlg (blue; G and H) or FasII (red; I). In contrast to controls, *nrg*^{14} mutant α'β' and αβ axons but not γ axons (I) project aberrantly straight to the α lobe tip, bypassing the MB pedunculus and lobes (asterisks). (J) Quantification of MARCM phenotypes (*n* = 31, 11, 5, 131, 9, and 14, in the respective order of the genotypes indicated). (K) Schematic drawing of wild-type and *nrg*^{14} mutant axon trajectories in G–I.

Importantly, analysis of γ axon projections using a specific GAL4-driver line (NP21) demonstrated only minor alterations in lobe morphology in *nrg*^{849} mutants and no defects in *nrg*^{14}; P[*nrg*^{180}_*ΔC*] mutants (Fig. S1, D–F, H, and I).

Nrg enforces axon guidance into the MB pedunculus and lobes

To address potential functions of Nrg that may be masked by the hypomorphic nature of our extra- and intracellular mutations, we next analyzed MB neurons lacking all Nrg using the mosaic analysis with a repressible cell marker (MARCM) technique (Lee and Luo, 1999). Axons of *nrg*^{14} single cell mutant clones never failed to grow out or to enter the pedunculus, and we observed only minor branching defects in agreement with prior observations (Fig. 2, A–C, J; Goossens et al., 2011). To address whether Nrg is potentially required for the coordination of larger population of axons or for the interaction between axons of different identity, we next generated NB clones that

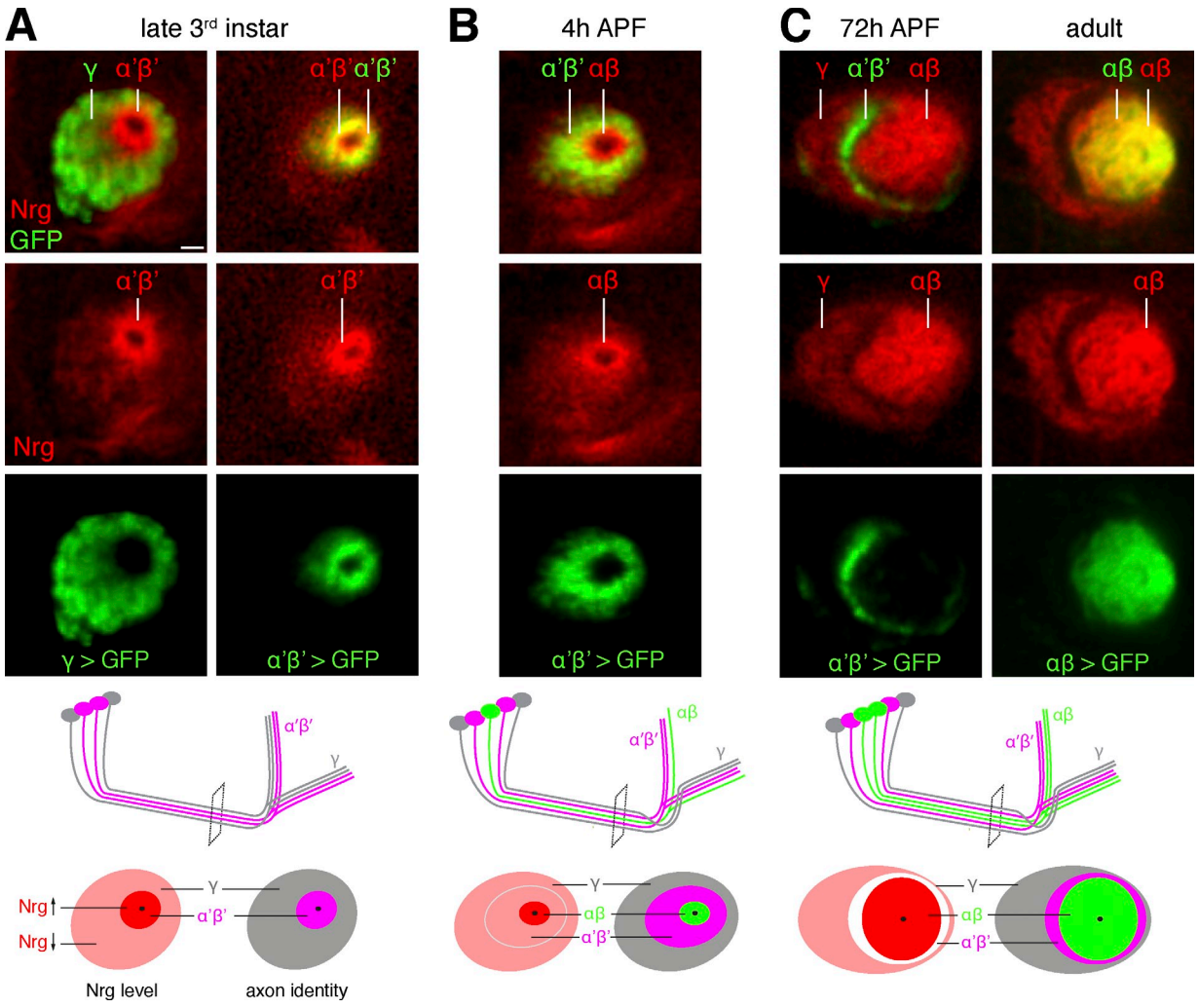

Figure 3. **Nrg is dynamically expressed during MB development.** (A–E) Analysis of Nrg^{180} expression (red) in MB pedunculus cross-sections at the position indicated in the schematics using cell type–specific Gal4 lines driving mCD8-GFP (green). The following Gal4-driver lines were used: *NP0021* (γ neurons), *c305a* (α′β′ neurons), and *c739* (αβ neurons). Bar, 2.5 µm. (A) In late third instar larvae, high levels of Nrg are present in α′β′ axons, which are surrounded by γ axons expressing lower Nrg levels. (B) At early pupal stages (4 h after puparium formation [APF]), Nrg is down-regulated in α′β′ axons and now highly expressed in *c305a*-Gal4–negative αβ axons. (C) In late pupal and adult stages, Nrg is down-regulated in α′β′ axons but remains expressed at high levels in αβ and at lower levels in γ axons.

either included only αβ neurons, both α′β′ and αβ neurons, or all three subtypes of MB neurons (Fig. 1 A). Interestingly, the majority of αβ NB clones did not show any alteration of axonal projections (Fig. 2, D, E, and J). However, in ∼20% of these clones, we observed defects including the formation of ball-like structures below the calyx resembling the phenotype of hypomorphic *nrg* mutations (Fig. 2, F and J). In contrast, 78% of NB clones that included α′β′ neurons in addition to αβ neurons showed striking defects in MB development, with mutant α′β′ and αβ axons projecting straight to the tip of the α-lobes. In these cases, axons take a shortcut and circumvent their normal path through the pedunculus and the lobes (Fig. 2, G–K). Interestingly, mutant γ axons projected appropriately through the pedunculus to the lobes (Fig. 2 I). These data indicate that Nrg is not required in single axons navigating into the MB structure but is required within populations of α′β′ and/or pioneering αβ axons that likely mediate an interaction between these two distinct axonal populations.

Dynamic expression of Nrg during MB development

To gain insights into how Nrg coordinates the guidance of α′β′ and αβ axons into the pedunculus, we next examined the expression pattern of Nrg during MB development. At late larval stages when the first α′β′ axons intercalate in between γ neurons at the center of the pedunculus (Fig. 1 A), we observed low levels of Nrg in γ axons but high levels within the axons of α′β′ neurons especially at the interface with the γ axons (Fig. 3 A). During early pupal development (4 h after pupal formation [APF]), when αβ axons start to intercalate in between α′β′ axons at the center of the pedunculus, we observed a striking switch in Nrg expression: the highest levels were now present in ingrowing αβ axons at the boundary to α′β′ axons, which now expressed lower levels of Nrg (Fig. 3 B). During pupal and adult development, Nrg expression remained high in αβ axons and low in γ axons but was completely down-regulated in α′β′ axons (Fig. 3 C). Thus, throughout development Nrg expression is regulated in a

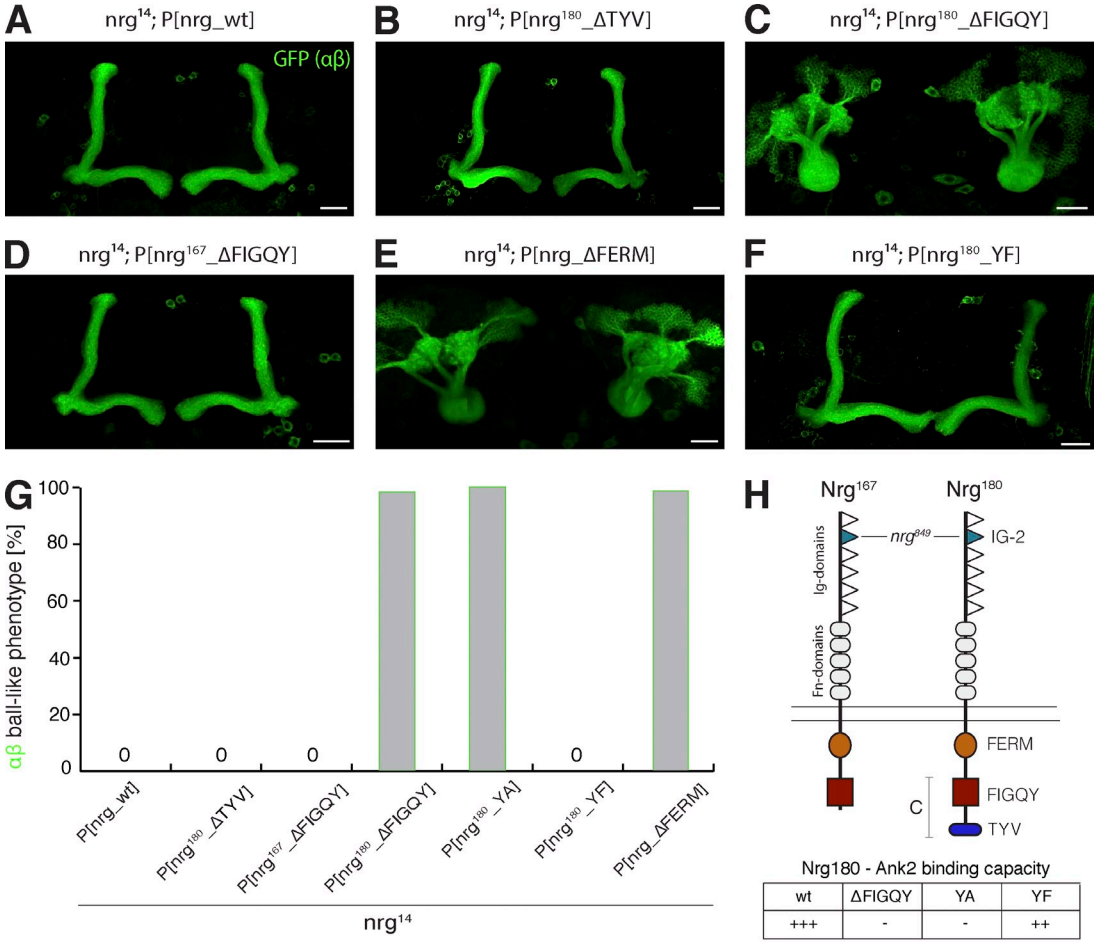

Figure 4. **Intracellular FIGQY and FERM domains are required for MB development.** (A–F) αβ neurons marked by mCD8-GFP expression (*c739*-Gal4). Frontal projections of the anterior (A, B, D, and F) or of the entire brain are shown (C and E). Bars, 20 µm. (A) In *nrg*^{14}*;* P[*nrg_wt*] control animals, αβ axons form medial and vertical lobes in the anterior brain. (B) The binding motif for PDZ domain containing proteins (TYV) of Nrg^{180} is not required for MB axon pathfinding. (C and D) Deletion of the FIGQY motif of Nrg^{180} but not of Nrg^{167} results in aberrant axonal accumulations in the posterior brain and absence of anterior αβ lobes. (E) Deletion of the FERM protein–interacting domain results in aberrant projections and an absence of αβ lobes. (F) A YF mutation within the FIGQY motif of Nrg^{180} restores MB development but β lobes were fused at the midline (see also Fig. S2). (G) Quantification of aberrant ball-like projections of αβ axons analyzed using FasII or c739>mCD8-GFP (*n* = 44, 66, 80, 81, 78, 84, and 56, in the respective order of the genotypes indicated). (H) Schematic model of the domain structure of the Nrg isoforms Nrg^{180} and Nrg^{167}. The positions of the extracellular mutation *nrg*^{849} and of intracellular domains are indicated. A summary of the in vitro Nrg–Ank2 interaction data from Enneking et al. (2013) is displayed.

dynamic, cell type–specific manner, with the highest expression levels present in axons that replace previously born neurons of different identity at the center of the pedunculus.

Together these data demonstrate that Nrg is required to guide MB axons into the pedunculus and lobes. The dynamic expression pattern suggests that Nrg potentially controls selective adhesion between populations of axons of different identity.

The intracellular FIGQY and FERM domains are required for MB development

Based on the striking phenotype caused by the partial deletion of the cytoplasmic tail of Nrg (Fig. 1, D, G, and H), we next aimed to identify the essential intracellular protein domains and their potential interaction partners. The C terminus of Nrg contains three major intracellular motifs: a FERM-interacting domain providing a potential link to the actin cytoskeleton shared by the neuronal (Nrg^{180}) and nonneuronal isoform of Nrg (Nrg^{167}), isoform-specific Ankyrin-interacting domains (FIGQY), and an Nrg^{180}-specific PDZ-interacting domain (Fig. 4 H). To directly assess the requirements of these domains, we analyzed genomic rescue constructs carrying domain-specific deletions (see Materials and methods; Enneking et al., 2013). Importantly, all constructs rescued the embryonic lethality associated with the *nrg*^{14}-null mutation, enabling analysis of adult MBs. It has been previously demonstrated that the C-terminal PDZ-interacting domain can bind to the MAGUK protein Polychaetoid (Pyd) in vitro, and genetic interaction studies indicated relevance of this interaction for MB development (Goossens et al., 2011). However, rescue constructs lacking the core residues of the C-terminal PDZ-interacting domain (ΔTYV) that mediate binding to Pyd completely restored MB development, thus excluding an essential requirement of this domain (Fig. 4, A, B, and G). In contrast, absence of the Ankyrin interaction domain (ΔFIGQY) in the neuronal isoform Nrg^{180} but not in Nrg^{167} isoform led to the formation of aberrant ball-like αβ axon projections in the posterior brain (Fig. 4, C, D, and G). Strikingly, we observed an identical phenotype when the FERM–protein interaction domain was deleted (ΔFERM; deletion of amino acids 1156–1166; Fig. 4,

E and G). Thus, two distinct and potentially independent intracellular Nrg protein–protein interaction motifs are essential for MB development in vivo.

Nrg–Ankyrin2 (Ank2) and Nrg–Moesin associations control MB axon guidance

Phosphorylation of the tyrosine residue within the FIGQY motif negatively regulates the binding of L1 protein family members to Ankyrins (Garver et al., 1997; Tuvia et al., 1997). This effect can be mimicked by specific amino acid substitutions, which alter binding to Ank2 and change the mobility of L1CAM in vitro (Gil et al., 2003) or of Nrg in axons in vivo (Enneking et al., 2013). Similar to *nrg*^{14}*;* P[*nrg*^{180}*_ΔFIGQY*] mutant animals, a point mutation abolishing the Nrg–Ank2 interaction (YA) failed to rescue MB development (*nrg*^{14}*;* P[*nrg*^{180}*_YA*]; Fig. 4 G). In contrast, a point mutation inducing a constitutive Nrg–Ank2 interaction by rendering the tyrosine nonphosphorylatable (YF) efficiently restored MB axon projections into the pedunculus and the anterior lobes (*nrg*^{14}*;* P[*nrg*^{180}*_YF*]; Fig. 4, F and G). Interestingly, in YF mutants we observed minor defects in α lobe tip innervation and a partial fusion of the β lobes from the two brain hemispheres, which indicates that a dynamic regulation of the Nrg–Ank2 interaction is essential for normal lobe morphogenesis (Fig. 4 F; and Fig. S2, A–C). To independently test the requirement of a cytoplasmic Nrg–Ank2 association, we performed genetic interactions assays. The *nrg* allele *nrg*^{305} significantly reduced expression of both Nrg isoforms (Fig. 5 E) and caused MB lobe formation defects in 65% of brain hemispheres but only mildly affected axonal projection into the pedunculus (Fig. 5, A and D). Strikingly, removal of one copy of *ank2* (using the *ank2*-null allele *ank2*^{518}) in hemizygous *nrg*^{305} mutant animals resulted in a dramatic enhancement of the phenotype, with 80% of αβ axons now failing to enter the pedunculus (Fig. 5, C and D). Because the *ank2*^{518} allele did not impair MB development in heterozygosity (Fig. 5, B and D), these data are consistent with the Nrg–Ank2 interaction contributing to MB axon guidance (Fig. 5 J).

We used a similar approach to identify potential binding partners of the Nrg FERM–protein interaction domain. Prime candidates are proteins of the ERM protein family that are represented by a single member in the *Drosophila* genome, Moesin (McCartney and Fehon, 1996; Adams et al., 2000). However, it has been demonstrated that Nrg can also be present in a complex with the related 4.1 protein family member Coracle (Genova and Fehon, 2003). Therefore, we tested the requirements of both Moesin and Coracle for Nrg-dependent MB development using previously characterized RNAi constructs (Ramel et al., 2013; Gardiol and St Johnston, 2014). While MB-specific RNAi-mediated knockdown of Coracle did not result in any MB defects, knockdown of Moesin resulted in lobe projection defects (Fig. 5, G and I), which indicates that Moesin is required for MB development. Indeed, knockdown in MB neurons of Moesin but not of Coracle in hemizygous *nrg*^{305} mutant animals resulted in a striking enhancement of the *nrg*^{305} mutant phenotype, with almost 100% of αβ axons failing to enter the pedunculus (Fig. 5, H and I). Together, these data identify Moesin and Ank2 as likely intracellular interaction partners of Nrg during MB axon guidance (Fig. 5 J).

Trans-axonal control of pedunculus and lobe formation

Based on the dynamic expression of Nrg at the border between ingrowing and substrate axons, we hypothesized that Nrg acts as a homophilic CAM to mediate axon–axon interactions during pedunculus entry. To test this hypothesis and to investigate potential cell type–specific requirements of the different Nrg domains, we used the UAS-Gal4 system to express wild-type Nrg^{180} selectively in either α′β′ or γ neurons in the background of the domain-specific *nrg* mutants. In these animals, wild-type Nrg^{180} will be present only in substrate (γ) or ingrowing axons (α′β′) while all other MB neurons express mutant Nrg. This enables a direct analysis of cell type–specific axo–axonal interactions mediated between wild-type and mutant Nrg proteins. In *nrg*^{14}*;* P[*nrg*^{180}*_ΔFIGQY*], expression of wild-type Nrg^{180} in ingrowing α′β′ neurons was sufficient to rescue pedunculus entry and lobe formation of α′β′ axons (Fig. 6, A–C and E). Strikingly, in these animals we also observed an almost complete rescue of αβ axons that only express mutant Nrg lacking the FIGQY domain (Fig. 6, A′–C′ and F). Similarly, expression of wild-type Nrg^{180} in γ neurons was sufficient to rescue projections of mutant α′β′ neurons (Fig. 6, D and E). These data demonstrate that the presence of wild-type Nrg^{180} in either substrate or ingrowing axons is sufficient to compensate for the absence of the Nrg FIGQY protein interaction motif within the interacting axonal population and indicates that Nrg acts as a homophilic CAM during these axo–axonal interactions. Interestingly, in animals expressing wild-type Nrg^{180} only in γ neurons, we also observed a partial rescue of αβ projections into the pedunculus, but the axons failed to innervate αβ lobes (Fig. 6, D′ and F). Analysis of the axonal projections within the pedunculus revealed a severe perturbation of axonal layer organization, with mutant αβ neurons now directly contacting wild-type Nrg^{180}-expressing γ neurons (Fig. 6 D, arrow), a phenotype never observed in control animals (Fig. 6 A). Thus, mutant αβ axons likely used wild-type Nrg-expressing γ axons as a substrate to enter the pedunculus. However, at the end of the pedunculus these mutant αβ axons failed to use the *nrg*^{14}*;* P[*nrg*^{180}*_ΔFIGQY*] mutant α′β′ lobes (Fig. 6, D and D′) as a template and therefore could not form αβ lobes. These data are consistent with the two axonal populations also interacting in an Nrg-dependent manner at this choice point during lobe development.

We next addressed whether a similar trans-axonal rescue is possible in animals lacking the intracellular FERM protein interaction domain of Nrg. Surprisingly, and in contrast to *nrg*^{14}*;* P[*nrg*^{180}*_ΔFIGQY*] mutant animals, expression of Nrg^{180} in either ingrowing (α′β′) or substrate (γ) neurons in *nrg*^{14}*;* P[*nrg_ΔFERM*] mutant animals failed to restore the α′β′ or αβ axonal projection patterns (Fig. 6, G–I, G′–I′, K, and L). However, expression of Nrg^{180} in all MB neurons almost completely restored MB development with only minor αβ lobe defects (Fig. 6 J, J′, K, and L). Thus, in contrast to the FIGQY domain, the FERM protein interaction domain is required simultaneously in both ingrowing and substrate neurons to allow pedunculus entry of α′β′ and αβ axons.

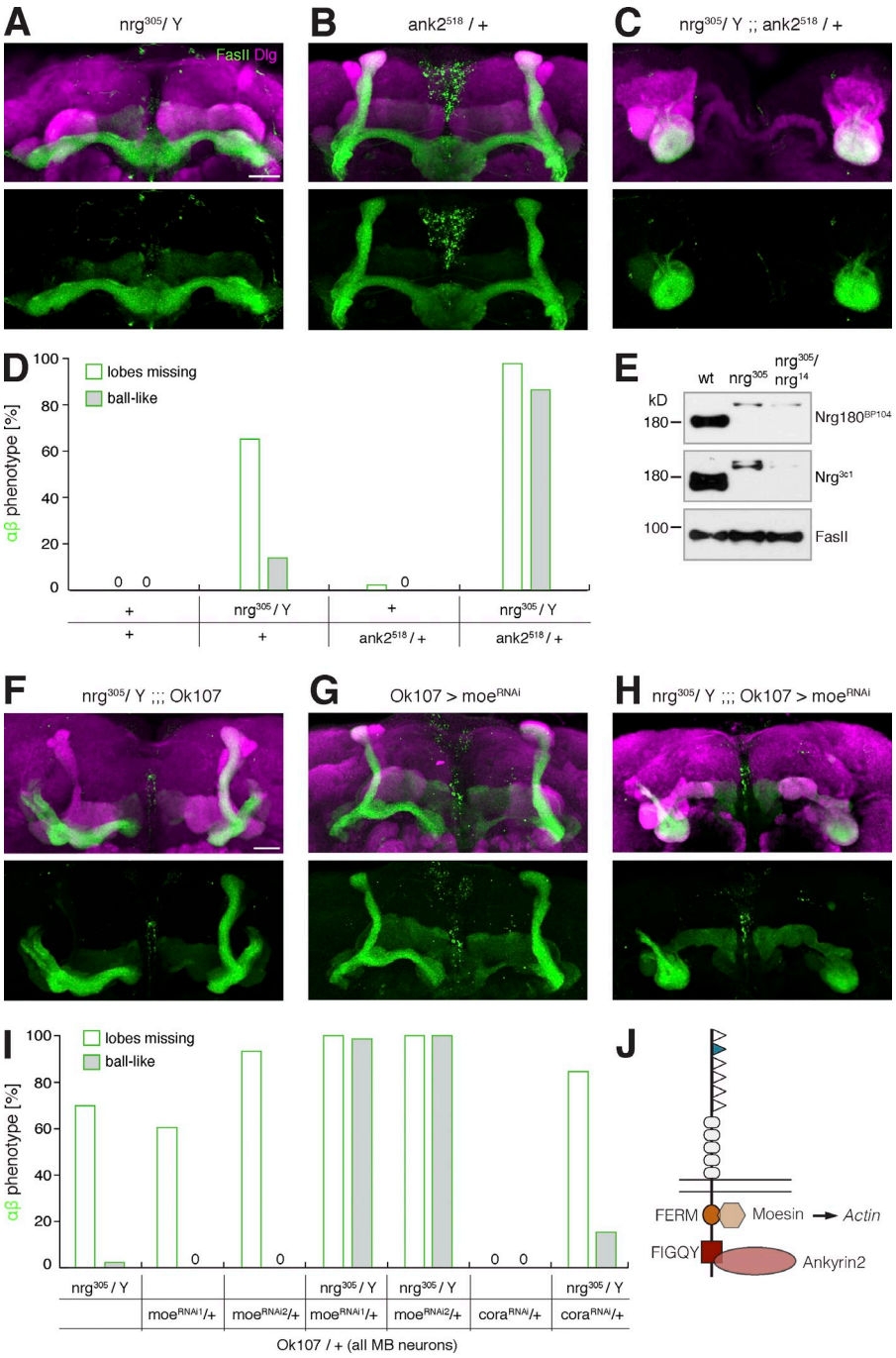

Figure 5. **Nrg–Ank2 association controls MB axon guidance.** (A–C and F–H) Frontal projections of the anterior (A, B, F, and G), posterior (C), or entire (H) region of the MBs visualized using FasII (green, αβ axons) and Dlg (magenta, neuropil). Bars, 20 µm. (A) In hemizygous *nrg*^{305} mutant animals, αβ axons display branching and lobe formation defects but rarely fail to project through the pedunculus. (B) Heterozygous mutations of *ank2* (*ank2*^{518}/+) do not affect MB development. (C) Removal of one copy of *ank2* in hemizygous *nrg*^{305} mutant animals severely enhances the MB axon phenotype, with MB axons failing to enter the pedunculus and forming aberrant ball-like structures in the posterior brain. (D) Quantification of the αβ axon phenotype assayed using FasII (*n* = 60, 43, 42, and 44, respectively, in the order of the genotypes given). (E) Western blot analysis of Nrg expression in larval brain extracts. The *nrg*^{305} GFP-trap mutation reduces protein expression of both Nrg^{180} and Nrg^{167}. (F) *nrg*^{305} mutant animals display mild axonal defects including branching and lobe formation defects. (G) Knockdown of Moesin in MB neurons causes defects in αβ axon branching and lobe formation but does not lead to aberrant axonal accumulations in the posterior brain. (H) Knockdown of Moesin in MB neurons in *nrg*^{305} mutant animals results in a dramatic enhancement of the phenotype compared with both individual genotypes, with MB axons now forming aberrant ball-like structure in the posterior brain. (I) Quantification of αβ axon phenotype using FasII (*n* = 43, 38, 30, 72, 26, 26, and 26, respectively, in the order of the genotypes indicated). (J) Schematic model indicating essential Nrg interaction partners.

We then analyzed the cell type–specific requirements of extracellular adhesion using the *nrg*^{849} mutation, which causes an S213L exchange within the second Ig domain. It was previously reported that this mutation completely abolished Nrg-dependent homophilic cell–cell interactions in a *Drosophila* S2 cell aggregation assay (Goossens et al., 2011). However, a complete loss of adhesive properties of the Nrg^{S213L} protein in vivo is not consistent with the observation that *nrg*^{849} mutant animals survived to adulthood while *nrg*^{14}-null and *nrg*$^{\Delta Ig3–4}$ mutants that completely lack the extracellular Ig domains 3 and 4 die as late embryos (Bieber et al., 1989; Enneking et al., 2013). Interestingly, the potential analogous human L1CAM disease mutation H210Q (Jouet et al., 1994; Vits et al., 1994) reduces homophilic L1-L1 adhesion but efficiently binds to wild-type L1 protein (Castellani et al., 2002). To address potential association between Nrg^{S213L} and wild-type Nrg, we performed S2 cell aggregation assays using transient transfection of fluorescently tagged proteins. While expression of Nrg lacking Ig domains 3/4 did not induce cell cluster formation, we observed efficient clustering of cells expressing GFP-tagged Nrg^{S213L} (Fig. S3). This indicates at least partial homophilic binding activity consistent with the hypomorphic nature of the *nrg*^{849} mutation in vivo. In addition, we observed efficient association between Nrg^{S213L} and wild-type Nrg^{180}-expressing cells, demonstrating that mutant and wild-type proteins can form functional homophilic interactions (Fig. S3). Based on these results, we next tested in vivo whether formation of a trans-axonal

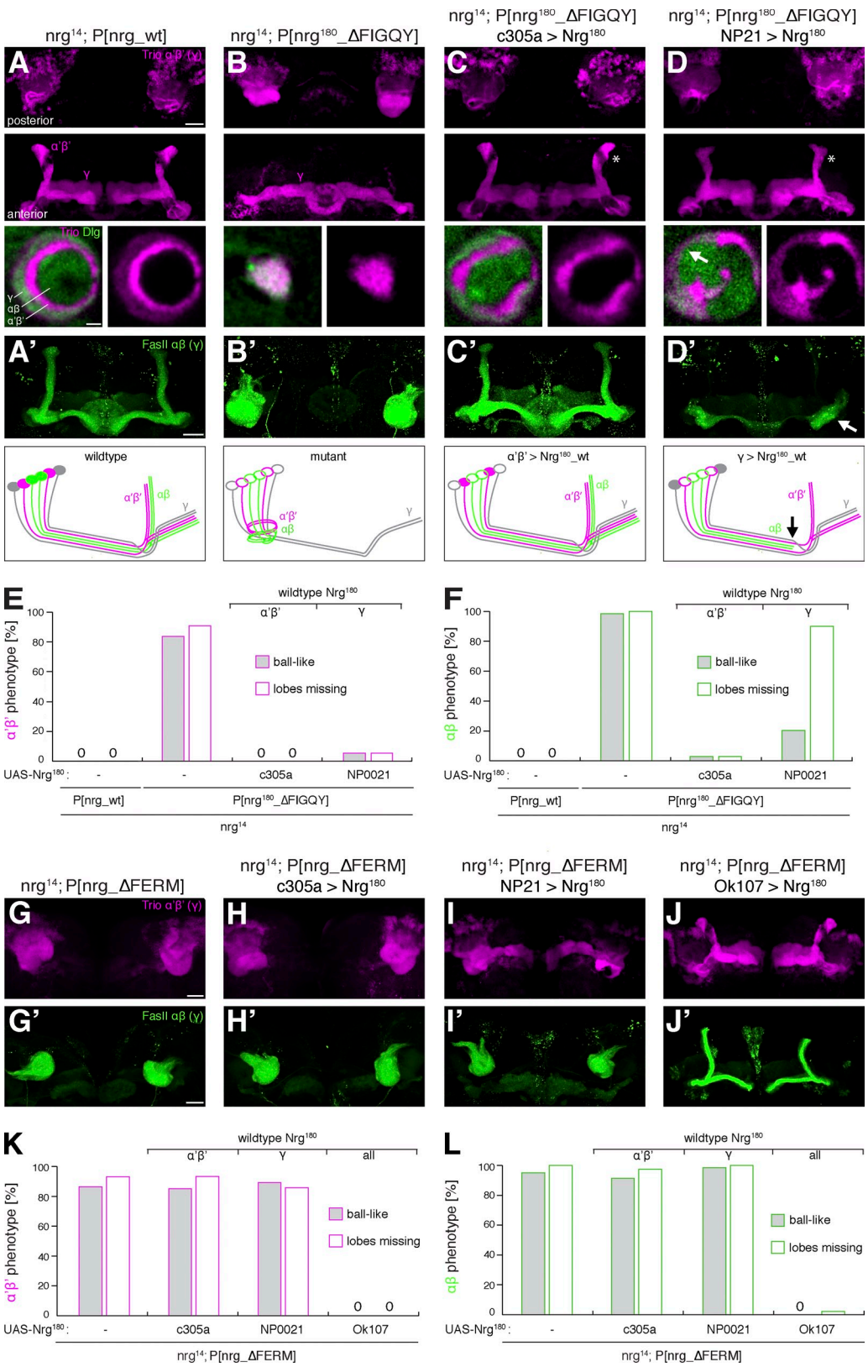

Figure 6. **Trans-axonal control of pedunculus and lobe formation.** (A–D) Frontal projections of posterior (top) and anterior regions (middle) of MBs marked by Trio (magenta; α′β′, high; and γ, low). Bottom panels show cross-sections of the pedunculus stained for Trio (magenta) and Dlg (green). Bars: (top) 20 µm; (bottom) 2.5 µm. (A′–D′) Top panels show frontal projections of entire MBs marked by FasII (green; αβ, high; and γ, low). Schematics summarize axonal projection phenotypes. Bars, 20 µm. (A) In control *nrg*^{14}; P[*nrg_wt*] animals, Trio-positive axons of α′β′ and γ neurons project into anterior lobes. Within the pedunculus, γ, α′β′, and αβ axons are clearly segregated into distinct concentric layers. (A′) αβ axons form medial and vertical lobes. (B) In *nrg*^{14}; P[*nrg*^{180}*_ΔFIGQY*] mutant animals, α′β′ axons fail to project into the pedunculus and form aberrant ball-like projections in the posterior brain. Only γ neurons (also Trio positive; imaged at higher gain settings compared with controls) form anterior lobes. (B′) αβ axons fail to form anterior lobes and form aberrant projections in

complex between wild-type and mutant Nrg^{S213L} proteins may be sufficient to rescue MB development. Indeed, expression of wild-type Nrg only in α′β′ neurons efficiently restored pedunculus projections and formation of α′β′ lobes in *nrg*^{849} mutants (Fig. 7, A–C and E). However, later ingrowing mutant αβ neurons failed to use these wild-type Nrg^{180}-expressing neurons as a template, as indicated by the absence of αβ lobes (Fig. 7, C′ and F). Consistent with wild-type Nrg^{180} being required in the ingrowing neuronal subtype, we did not observe any rescue of mutant α′β′ or αβ MB axonal projections when wild-type Nrg^{180} was expressed in γ neurons using two different Gal4 lines (Fig. 7, D, D′, E, and F). Together, these rescue experiments revealed striking differential requirements of the extra- and intracellular domains of Nrg. These differences were particularly evident when comparing the α′β′ rescues in the different mutant backgrounds. The presence of wild-type Nrg^{180} in α′β′ neurons efficiently restored α′β′ but not αβ projections in *nrg*^{849} mutants, whereas it was sufficient to restore projections of both α′β′ and αβ neurons in *nrg*^{14}*;* P[*nrg*^{180}*_ΔFIGQY*] mutant animals (Fig. S4).

Cooperative control of Nrg-mediated axo–axonal interactions

Based on the trans-axonal rescues of *nrg*^{14}*;* P[*nrg*^{180}*_ΔFIGQY*] mutants, we hypothesized that a major function of the Ank2 interaction may be clustering of Nrg, a feature that in principle can be accomplished with equal efficacy from either side of a trans-axonal interaction. If Nrg mediated axon–axon interactions depend on the formation of Nrg clusters, we would predict intragenic complementation between the three *nrg* mutations despite their unique cell type–specific requirements. Strikingly, while we observed identical phenotypes for all three mutations when homo/hemizygous (Fig. 8, A–C and G), all trans-heterozygous combinations restored pedunculus entry and at least partially rescued lobe formation (Fig. 8, D–G). These results provide strong evidence that multimeric clusters mediate Nrg function in vivo. These data further demonstrate that the $Nrg^{\Delta FERM}$ protein is functional and that the intracellular FIGQY and FERM domains act independently of each other. The observed lobe formation defects in transheterozygous *nrg*^{849} and *nrg*^{14}*;* P[*nrg_ΔFERM*] mutants were consistent with the more essential requirements of these two protein domains (Fig. 8, F and G). Together, these data demonstrate that the extra- and intracellular Nrg protein–protein interaction domains act in a cooperative manner during the cell type–specific axon–axon interactions necessary for the establishment of MB architecture (Fig. 8 H).

Discussion

Our combined analysis using targeted, domain-specific mutations of the *Drosophila* L1CAM homologue Nrg with cell type–specific rescues enabled us to unravel the cellular mechanisms controlling MB development and to gain insights into the general molecular mechanisms underlying CAM-mediated cell adhesion and axon guidance in vivo. At the cellular level, we provide evidence for the potential presence of an attractive signal at the tip region of MB lobes that guides MB axons to the anterior brain. Axon–axon interactions mediated by Nrg are necessary to enforce guidance of α′β′ and then αβ neurons through the pedunculus and along the lobes to their target to establish the characteristic layered and lobular organization of the MBs essential for learning and memory. At the molecular level, our data suggest that intracellular association with Ank2 and Moesin is independently required for the establishment of functional trans-axonal Nrg complexes and MB axon guidance in vivo. Our results demonstrate that CAM-mediated axon–axon interactions are tightly controlled by intracellular protein–protein interactions and enable the establishment of complex layered and lobular neuronal circuit architecture.

Nrg controls MB axon guidance

The analysis of MB axons lacking all Nrg revealed striking insights into the mechanisms controlling MB assembly. Our data show that Nrg is not essential for neurite extension or axon pathfinding of individual neurons or of small populations of neurons of equal identity. However, as soon as *nrg* mutant NB clones included neurons of two identities, we observed a dramatic alteration of axon trajectories. Instead of entering the pedunculus and following the lobe pathways, mutant axons projected directly to the final target, the tip of the α/α′ lobes. Together with our cell type–specific rescue data, these results indicate that Nrg is essential to mediate axon–axon interactions between axon populations of different identities to enforce and enable guidance through the MB structure. Furthermore, these data indicate that α/α′ lobes are the likely source of a long-range chemoattractive axon guidance signal. However, an alternative explanation may be that the shortcut pathway simply represents a permissive default trajectory. Wnt signaling represents a prime candidate to mediate MB axon guidance because it has been implicated in anterior–posterior guidance in both invertebrates and vertebrates (Lyuksyutova et al., 2003; Yoshikawa et al., 2003) and because the *wnt5* mutant phenotype shares similarities with the

the posterior brain. (C) Expression of wild-type Nrg^{180} in α′β′ neurons of *nrg*^{14}*;* P[*nrg*^{180}*_ΔFIGQY*] mutants restores anterior projections of α′β′ neurons. Minor perturbations of axonal layer organization are evident in the pedunculus. (C′) In these animals, projections of αβ mutant axons are also efficiently rescued and αβ lobes form next to the wild-type Nrg^{180}-expressing α′β′ lobes (asterisk in C). (D) Expression of wild-type Nrg^{180} in γ neurons of *nrg*^{14}*;* P[*nrg*^{180}*_ΔFIGQY*] mutants also rescues α′β′ projections. Pedunculus cross-sections reveal aberrant organization of axonal layers, with mutant αβ axons inappropriately in contact with γ axons (arrow). (D′) In these animals, αβ axons grow into the pedunculus to the pedunculus divide (heel, arrow) but fail to form medial or vertical lobes (note the altered appearance of α′β′ lobes in D due to the absence of αβ lobes, indicated by the asterisk). (E) Quantification of α′β′ phenotypes (*n* = 24, 55, 18, and 30, respectively, in the order of the genotypes indicated). (F) Quantification of αβ phenotypes (*n* = 44, 61, 69, and 36, respectively, in the order of the genotypes indicated). (G–J and G′–J′) Frontal projections of entire MBs. (G and G′) In *nrg*^{14}*;* P[*nrg_ΔFERM*] mutant animals, axons of α′β′ and αβ neurons form aberrant ball-like projections in the posterior brain and fail to form anterior lobes. (H and H′) Expression of wild-type Nrg^{180} in α′β′ neurons of *nrg*^{14}*;* P[*nrg_ΔFERM*] mutants does not rescue the MB phenotype. (I and I′) Expression of wild-type Nrg^{180} in γ neurons of *nrg*^{14}*;* P[*nrg_ΔFERM*] mutants does not rescue the MB phenotype. (J and J′) Expression of wild-type Nrg^{180} in all MB neurons efficiently rescues axonal projections. Bars, 20 µm. (K) Quantification of the α′β′ phenotypes (*n* = 44, 61, 28, 31, and 24, respectively, in the order of the genotypes indicated). (L) Quantification of the αβ phenotypes (*n* = 102, 82, 65, 48, and 30, respectively, in the order of the genotypes indicated).

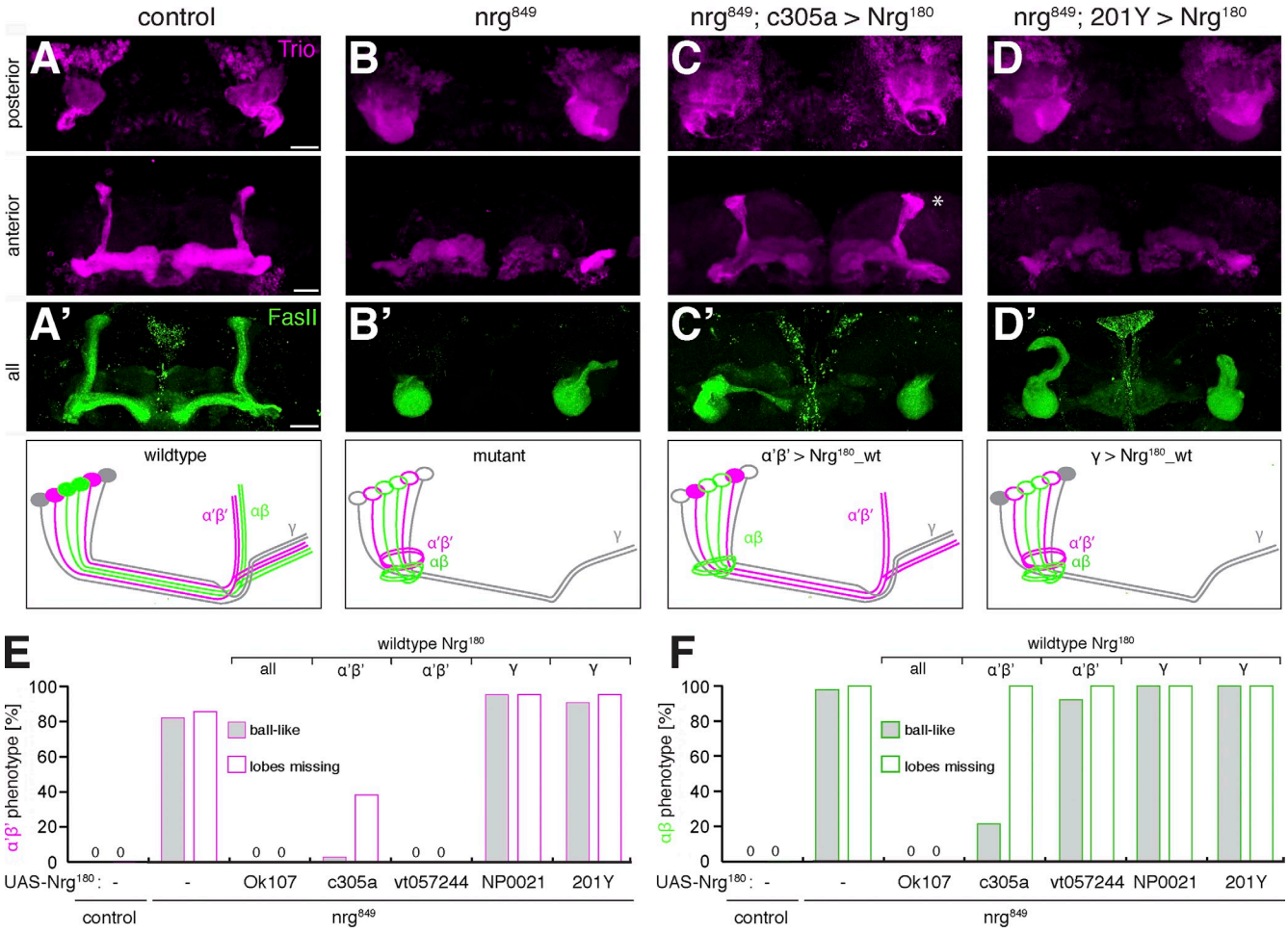

Figure 7. **Extracellular adhesion controls axonal intercalation.** (A–D) Anterior and posterior projections of α′β′ and γ neurons marked by Trio (magenta) are shown. (A′–D′) Top panels show entire MB projections of αβ axons marked by FasII (green). Schematics summarize the axonal phenotypes. (A and B) In contrast to control animals, in *nrg*^{849} mutant animals α′β′ axons fail to enter the pedunculus and form ball-like aggregates in the posterior brain. Medial γ lobe projections show minor defects. (B′) In mutant animals, αβ axons also fail to enter the pedunculus. (C) Cell type–specific expression of wild-type Nrg^{180} in α′β′ neurons of *nrg*^{849} mutant animals restores α′β′ lobular projections. (C′) No rescue of αβ projections was observed when using *vt057244*-Gal4; however, we frequently observed partial rescue of αβ axons into the pedunculus but no rescue of lobe formation despite presence of α′β′ lobes when using *c305a*-Gal4. (D and D′) Expression of wild-type Nrg^{180} in γ neurons of *nrg*^{849} mutant animals does not rescue α′β′ or αβ projections. (E and F) Quantification of α′β′ (E) and αβ (F) axon phenotypes. Rescue data are presented using Gal4 drivers expressing wild-type Nrg^{180} in all MB neurons (*Ok107*-Gal4), α′β′ neurons (*c305a*-Gal4 and *vt057244*-Gal4), or γ neurons (*NP0021*-Gal4, *201Y*-Gal4; *n* = 26, 28, 20, 34, 36, 21, and 43 for E and *n* = 60, 46, 20, 28, 38, 28, and 44 for F, in the respective order of the genotypes indicated). Bars, 20 µm.

nrg MB phenotype (Grillenzoni et al., 2007). Uncoupling extracellular guidance signaling from the force-generating cytoskeletal machinery by mutating *rac* genes also resulted in a failure of axons to enter the pedunculus (Ng et al., 2002), which indicates that pedunculus entry represents a key choice point for α′β′ and αβ MB axons.

Homophilic Nrg–Nrg complexes control axo-axonal interactions

At the molecular level, our study provides mechanistic insights into the in vivo requirements of protein–protein interaction domains of CAMs during contact-dependent axon guidance. We propose a three-step process necessary for the formation of functional Nrg complexes during axo–axonal interactions.

First, adhesive contact is established by a homophilic Nrg interaction between ingrowing (α′β′) and substrate (γ) axons. We provide evidence that establishment of this inter-subtype axonal interaction requires active competition for binding partners and directly correlates with the adhesive properties of Nrg. Similar to the potential analogous human L1CAM disease mutation H210Q (Jouet et al., 1994; Vits et al., 1994; Castellani et al., 2002), and in contrast to a prior report (Goossens et al., 2011), we demonstrate that mutant Nrg^{S213L} (*nrg*^{849}) only partially impairs extracellular adhesion and can efficiently bind to wild-type Nrg (Nrg^{wt}). Our cell type–specific rescues demonstrated that expression of Nrg^{wt} in ingrowing but not in substrate neurons restores pedunculus entry of α′β′ axons in *nrg*^{849} mutants. Thus, Nrg^{wt} of ingrowing axons can interact with and resolve axo–axonal adhesion mediated by Nrg^{S213L} present on substrate axons. In contrast, in the reverse case mutant Nrg^{S213L} on ingrowing axons cannot dissolve the strong adhesive connections between substrate neurons that are mediated by Nrg^{wt}. Identical mechanisms also control the interactions between α′β′ and αβ neurons (Fig. S4). Consistent with this hypothesis, we

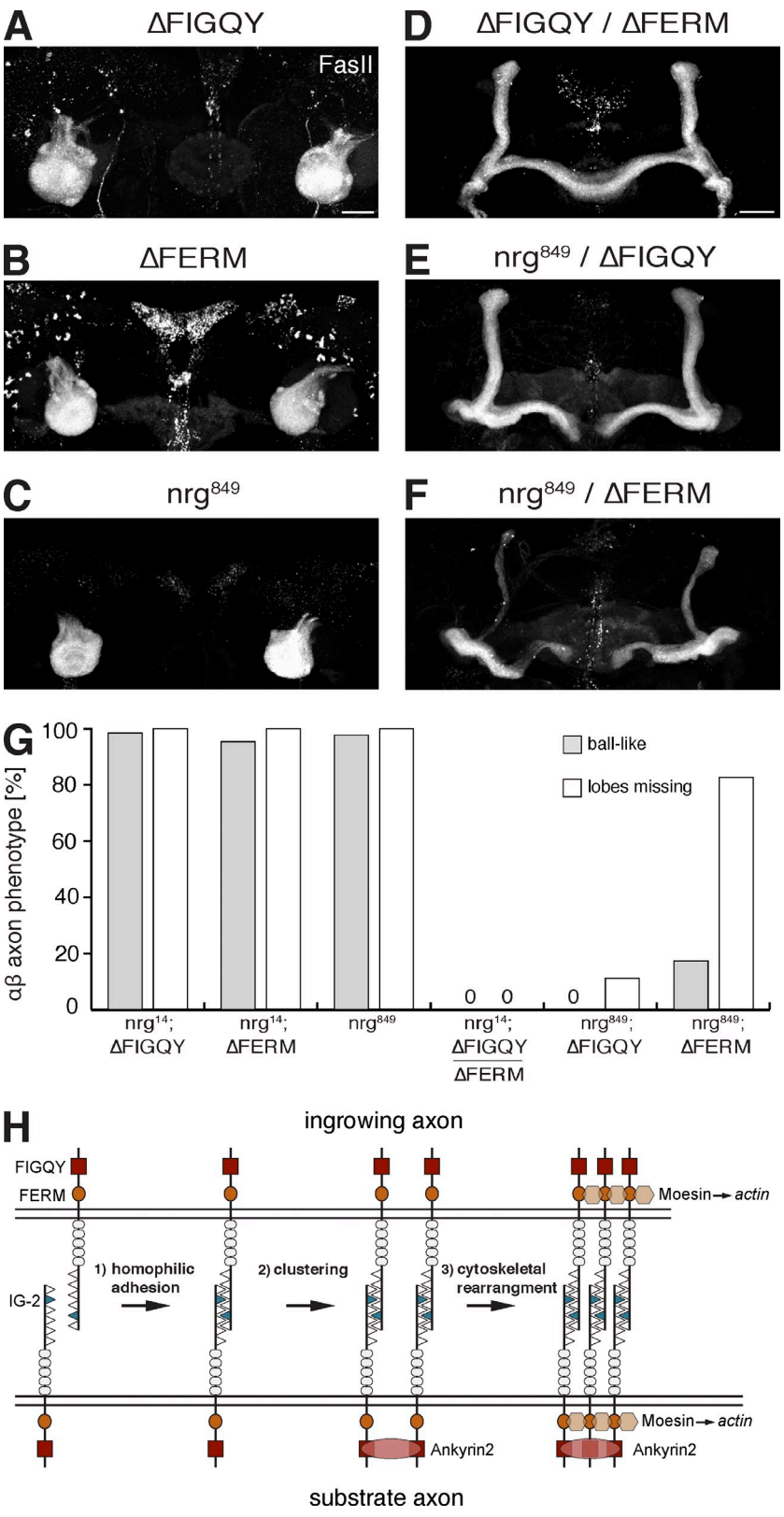

Figure 8. **Cooperative control of Nrg-mediated trans-axonal interactions.** (A–F) Frontal projections of the entire MBs (A–C) or only anterior regions (D–F). αβ axons are marked by FasII (white). Bars, 20 µm. (A–C) All hypomorphic *nrg* mutations result in identical αβ axon projection defects. (D–F) Transheterozygous combinations of two mutations almost completely restore MB projections. Aberrant β-lobe fusions were present in some ΔFIGQY/ΔFERM mutant animals (D), and severe perturbations of lobe formation were evident in animals transheterozygous for ΔFERM and nrg^{849} (F). (G) Quantification of the αβ phenotype (n = 63, 64, 46, 40, 36, 46, respectively, in the order of the genotypes indicated). (H) Model of the formation of functional Nrg clusters during trans-axonal interactions. Trans-axonal Nrg interactions are stabilized by Ank2-mediated clustering. Interactions with Moesin provide a link to the actin cytoskeleton that enables formation of stable complexes providing cellular adhesion.

observed a differential and dynamic expression of Nrg during MB development, with the highest levels of Nrg always present in the ingrowing axonal population (first α′β′ then αβ) especially at the boarder to the substrate axons (first γ then α′β′). The precise control of Nrg levels that likely reflect the strength of inter-axonal adhesion indicates that differential adhesion may not only mediate force-generating interactions but also contribute to the segregation of subtype-specific axonal population analogous to the adhesion-dependent sorting of synaptic fascicles observed in the *Drosophila* visual system (Schwabe et al.,

2014). It is important to note that an alternative explanation for the observed cell type–specific rescues of *nrg*^{849} mutant animals would be a disruption of potential cis interactions with signaling receptors, as demonstrated for other *nrg* mutations during sensory axon guidance (García-Alonso et al., 2000).

Second, we provide two lines of evidence that trans-axonal Nrg complexes have to be clustered and stabilized by intracellular interactions with the adaptor molecule Ank2. First, mutations in the intracellular FIGQY motif that selectively impair Ank2 binding (Enneking et al., 2013) display axon guidance phenotypes identical to mutations affecting the extracellular domain. In addition, loss of a single copy of *ank2* strongly enhanced the phenotype of a hypomorphic *nrg* mutation. Second, intracellular Ank2 association is sufficient on either side of the axon–axon interactions to restore pedunculus organization and lobe innervation. This bidirectional rescue provides strong evidence that Nrg acts as a homophilic CAM and indicates that Ank2-dependent cluster formation is mirrored across the inter-axonal interface, thereby resulting in the formation of stable trans-axonal Nrg complexes. These data are consistent with cell-based observations demonstrating selective recruitment of Ank2 to Nrg at sites of cell contact (Hortsch et al., 1998) and with the Nrg–Ank2 association controlling synapse maturation and function in a trans-synaptic manner (Enneking et al., 2013). The observation that constitutive Nrg–Ank2 association (YF mutation) disrupts lobe morphogenesis indicates that this interaction is potentially controlled by reversible phosphorylation of the FIGQY motif during normal MB development.

Third, we demonstrate that a second intracellular domain, the conserved juxtamembrane FERM protein interaction domain, is equally important and, in contrast to the FIGQY motif, required simultaneously in both axonal populations. Furthermore, using genetic interaction assays, we identify *Drosophila* Moesin as the likely interaction partner that provides direct association with the actin cytoskeleton. This is consistent with prior studies demonstrating that binding to ERM proteins enables coupling of L1CAM to the retrograde F-actin flow during neurite extension in vitro (Sakurai et al., 2008) and is required for axon branching in culture (Cheng et al., 2005). The simultaneous requirement in both ingrowing and substrate neurons indicates that the Moesin–F-actin link provides essential and unique functions in both axonal populations and does not simply serve as a static link to the cytoskeleton.

The striking intragenic complementation between the three *nrg* mutations that cause identical phenotypes provides compelling evidence that Nrg acts as a multimeric complex in vivo and that the two intracellular domains contribute independently to Nrg-mediated MB axon guidance. In principle these results are consistent with the intracellular Ank2 and Moesin–actin interaction contributing to forward movement through substrate–cytoskeletal coupling, as proposed using cell culture models (Suter et al., 1998; Gil et al., 2003). However, the absence of a neurite outgrowth phenotype in single-cell MARCM clones argues that in this in vivo system the main role of Nrg is likely the precise coordination of axon–axon interactions between axonal populations of different identity.

Our data are consistent with prior studies speculating that the later born axonal populations (αβ) follow pioneer tracts of different identity (α′β′) during MB lobe formation (Wang et al., 2002; Boyle et al., 2006; Bates et al., 2010; Shin and DiAntonio, 2011). We now identify essential requirements for trans-axonal Nrg interactions between γ-α′β′ and α′β′-αβ neurons, respectively, during pedunculus entry and lobe formation. This is best highlighted in the γ cell type–specific rescue experiments in *nrg*^{14}*; P[nrg*^{180}*_ΔFIGQY]* mutants (Fig. 6, D, D′, and F). In these experiments, the larval γ lobes (before pruning) that expressed wild-type Nrg served as a substrate for α′β′ axons to project into the pedunculus and likely the lobes as well. Consistent with the requirement for a functional Nrg–Ank2 association on at least one side of the axon–axon interactions, these mutant α′β′ axons could not serve as a functional substrate for mutant αβ axons. αβ axons likely used γ axons aberrantly to grow into the pedunculus but failed to grow into lobes due to the absence of a wild-type Nrg substrate. Based on these results, it is interesting to speculate that pioneering γ neurons use glia cells as a substrate for the initial projections into anterior lobes. Indeed, we observed small alterations in γ projections in *nrg*^{849} and *nrg*^{14}*;* P[*nrg_ΔFERM*] mutants that affect both the neuronal and the glial Nrg isoform (Nrg180 and Nrg167, respectively) but not in *nrg*^{14}*;* P[*nrg*^{180}*_ΔFIGQY*] mutants, which is consistent with the Nrg–Ank2 association being sufficient on either side of the Nrg–Nrg interface.

In addition, the disruption of pedunculus architecture in *nrg*^{14}*; P[nrg*^{180}*_ΔFIGQY]* mutant animals expressing Nrg^{wt} only in γ neurons (Fig. 6 D) indicates that Nrg participates in the establishment and maintenance of cell type–specific axonal layer organization. However, additional CAMs must contribute to axonal subtype segregation, as we observed a clear segregation based on axonal identity in all hypomorphic *nrg* mutants (Fig. 1, C and D). Dscam and FasII are expressed in subsets of MB neurons and required for MB development (Kurusu et al., 2002; Wang et al., 2002; Zhan et al., 2004). An attractive model would be that these CAMs act cooperatively during the establishment and maintenance of layered and lobular MB organization. Interestingly, analysis of CAM expression patterns in the fasciculus retroflexus identified a layer-specific and differential localization of all four vertebrate homologues of Nrg (L1, CHL1, NrCAM, and Neurofascin; Schmidt et al., 2014), which indicates potential conserved functions during axon–axon interactions that establish complex neuronal circuitry.

Finally, our data provide potential mechanistic insights into the molecular basis of the neurodevelopmental defects observed in L1 syndrome patients: partial agenesis of the corpus callosum (AgCC) and spinocerebellar projection defects (Wong et al., 1995). In patients with AgCC, callosal axons fail to cross the midline and instead form aberrant ipsilateral tracts partially maintaining topographic organization (Tovar-Moll et al., 2007). During normal development, callosal projections are established in a sequential manner depending on axon–axon interactions between axonal populations of different identities (Koester and O'Leary, 1994). Based on our data, an attractive hypothesis would be that decreased extracellular interactions between axons of different identity result in a failure to efficiently intercalate and project to appropriate targets on the contralateral side of the brain.

Table 1. **Primers used in this study**

Primers	Forward	Reverse
P[acman] FERM-GalK	5′-TCATCCTCTTCATCATCATCTGCATTATCCGACGCAATCGGGGCGGAAAGCCTGTTGACAATTAATCATCGGCA-3′	5′-TCTTCGGGATAATCCCGCCGGCCGTTGGCCAGCTCCCGATCGTGGACATCTCAGCACTGTCCTGCTCCTT-3′
P[acman] ΔFERM	5′-TGGCCCTGGCCTTCATCATCATCCTCTTCATCATCATCTGCATTATCCGACGGGAGCTGGCCAACGGCCGGCCGGGATTATCCCGAAGAGGGCGGATTCCA-3′	5′-TGGAATCCGCCCTCTTCGGGATAATCCCGCCGGCCGTTGGCCAGCTCCCGTCGGATAATGCAGATGATGATGAAGAGGATGATGATGAAGGCCAGGGCCA-3′
pUAST-Nrg^{S213L}	5′-CCGATTTCTACTATGCCTGCTTGGCCACCTCGGTGTTTCGCAG-3′	5′-CTGCGAAACACCGAGGTGGCCAAGCAGGCATAGTAGAAATCGG-3′
Check and seq primers		
P[acman] ΔFERM check	5′-TCCATGTACAGGATCAAGG-3′	5′-ACTCTAACCTGTATCGCCATC-3′
P[acman] ΔFERM seq	5′-CTTTAACACGGAGAGTGCCAC-3′	5′-GATTTTGGGACTTACGGTTGC-3′

Materials and methods

Fly stocks

All flies were maintained at 25°C on standard fly food except for RNAi experiments (29°C). The following strains were used in this study: *w*^{1118} (control), P(neoFRT)19A, *Ok107*-Gal4 (all MB neurons; Lee et al., 1999), *201Y*-Gal4 (αβ core and γ neurons; Aso et al., 2009), *c739*-Gal4 (α′β′ and γ neurons at late larval stages, only αβ neurons in adult animals; Fushima and Tsujimura, 2007), *c305a*-Gal4 (α′β′ neurons; Krashes et al., 2007), UAS-*mCD8-GFP*, *nrg*^{849}, *nrg*^{305} (*nrg*^{G00305}; GFP-trap affecting both isoforms of *nrg*: *nrg*^{167} and *nrg*^{180}), *nrg*^{14} (*nrg*^{1}, null allele), *tub*-FRT>Gal80>FRT, hsFlp^{86} (all from the Bloomington Stock Center), *NP0021*-Gal4 (*NP21*, γ neurons; Tanaka et al., 2008; Drosophila Genomics Resource Center, Kyoto Stock Center), *vt057244*-Gal4 (α′β′ neurons; Wu et al., 2013), UAS-moesin-RNAi (#1, 37917; #2, 33963; Ramel et al., 2013), UAS-coracle-RNAi (9788; Gardiol and St Johnston, 2014; all from Vienna Drosophila RNAi Center), *nrg*^{14}, and P(neoFRT)19A. P[*acman*] constructs used were: P[*nrg_wildtype*], P[*nrg*^{180}*_YF*] (Y1235F substitution in ORF of Nrg^{180}), P[*nrg*^{180}*_YA*] (Y1235A substitution in ORF of Nrg^{180}), P[*nrg*^{180}*_ΔFIGQY*] (deletion of aa 1231–1235 in ORF of Nrg^{180}), P[nrg^{180}_ΔC] (deletion of aa 1231–1302 of Nrg^{180} ORF), P[*nrg*^{180}*_ΔPDZ*] (deletion of aa 1300–1302 in ORF of Nrg^{180}), P[*nrg*^{167}*_ΔFIGQY*] (deletion of aa 1230–1234 in ORF of Nrg^{167}), UAS-*Nrg*^{180}*-EGFP* (C-terminal EGFP tagged Nrg^{180}; all described in Enneking et al., 2013), *ank2*^{518} (Pielage et al., 2008), *yw*, *tubGAL80*, *hsFlp*, and *FRT*^{19A}*;* UAS-*mCD8-GFP;;Ok107*-Gal4 (Lee and Luo, 1999). For the identification of Ok107-Gal4–positive animals (Fig. 3), UAS-*mCD8-GFP* was maintained in the background.

MARCM and flip-out analysis

P(neoFRT)19A and *nrg*^{14}, P(neoFRT)19A females were crossed to *y*, *w*, *tub-GAL80*, *hsFlp*, *FRT*^{19A}*;* UAS-*mCD8-GFP;;*Gal4-*Ok107* males. Embryos were collected for 4 h, and heat shocks were applied in a water bath at 37–38.5°C for 40–60 min at different developmental time points to generate either single neuron clones or NB clones containing different subtypes of MB neurons.

To perform flip-out experiments, *tub*-FRT>Gal80>FRT was combined with hsFlp^{86} and *201Y*-Gal4>UAS-*mCD8-GFP*. Heat shocks were applied at different pupal stages for 50–60 min in a water bath at 38°C.

Immunohistochemistry and microscopy

0–9-d-old adult male flies (females for MARCM analysis) were incubated in fixative for 3 h at 4°C (4% PFA, 0.2% Triton X-100), then washed three times for 30 min in PBST (0.2% Triton X-100) at RT before brain dissection. Brains of wandering third instar larvae were removed, fixed in 3.7% formaldehyde for 30 min, and subsequently washed in PBST (2% Triton X-100) four times for 20 min. Brains were incubated in primary antibody solution for 2–5 d and for 1–2 d in secondary antibody solution either at RT or 4°C. Antibodies were diluted in PBST (0.2% Triton X-100 for adult brains, 2% Triton X-100 for larval brains) and washed for three times for 30 min. The following antibodies were used in this study: rabbit anti-GFP (A6455, 1:1,000; Life Technologies), rabbit anti-Dlg (1:30,000; Pielage et al., 2011), rat anti-CD8a (MCD0800, 1:500; Life Technologies), mouse 1D4 (anti-FasII; 1:200), mouse anti-TRIO (9.4A, 1:200; Developmental Studies Hybridoma Bank), and Alexa Fluor 488–, 568–, and 647–coupled secondary antibodies (1:1,000; Life Technologies). Brains were mounted in Vectashield (Vector Laboratories). Images were captured using a laser scanning confocal microscope (LSM 700; Carl Zeiss; EC Plan-Neofluar 40×/1.3 NA oil M27 objective lens) or a laser scanning confocal microscope (TSC SPE; Leica; HCX Plan-Apochromat 20×/0.7 NA IMM CORR CS and HCX Plan-Apochromat 40×/1.25–0.75 NA oil CS objective lenses). Images were acquired at RT using Zen Black 2012 (Carl Zeiss) and LAS acquisition software (Leica) and processed using Imaris (Bitplane) and Photoshop software (Adobe).

Quantification of phenotypes

In adults, αβ axon phenotypes were quantified using FasII/Dlg staining or *c739*-Gal4-driven membrane-tethered GFP. Brain hemispheres were scored as "ball-like" when pedunculus projections were minimal or nonexistent and the majority of axons accumulated in the posterior brain. Brain hemispheres were scored as "lobes missing" when αβ lobes were absent or only minor projections were present. α′β′ axon phenotypes were assessed using Trio staining or membrane-tethered GFP driven by α′β′-specific Gal4 driver lines. "Ball-like" quantifications indicate aberrant projections below the calyx and "lobes missing" indicates the absence of α′ lobes. During the analysis of *nrg*^{14}*;* P[*nrg_ΔFERM*] mutants, we observed significant rates of nondisjunction, and X/0 animals were discarded based on eye color differences at adult hatching. Larval MBs were scored as "ball-like" based on aberrant axonal accumulations in the posterior brain marked by *c739*-Gal4–driven mCD8-GFP. Thinner γ lobes marked by *NP0021*-Gal4>mCD8-GFP in the anterior brain were scored as "lobe defects." *n* indicates the number of analyzed MBs. The two brain hemispheres were independently quantified. The following genotypes were used as controls: *w*^{1118} (Fig. 1 and Fig. 7, A and E), P(neoFRT)19A (Fig. 2, Fig. 7 F, and Fig. 5 D), and *nrg*^{14}*;* P[*nrg_wt*] (Fig. 7 A′, Fig. S1, and as indicated).

Generation of *nrg* constructs

Generation of the pUASt-*nrg*^{S213}*-EGFP*, pUASt-*nrg180-mCherry*, and *nrg_ΔFERM* P[acman] constructs was performed according to Enneking et al. (2013). In brief, the full-length *nrg*^{180} ORF was amplified and cloned into the pENTRY vector via TOPO cloning (Life Technologies). Point mutations were introduced into pENTRY clones using the QuikChange II site-directed mutagenesis kit (Agilent Technologies). Final constructs were shuffled into tagged pUASt vectors (Enneking et al., 2013) using Gateway technology (Life Technologies). To generate the *nrg_ΔFERM* constructs, the wild-type *nrg* P[acman] construct was modified using *galK*-mediated recombineering as described previously (Enneking et al., 2013). aa 1156–1166 of the open reading frame of Nrg180 were first replaced with a *galK* encoding construct. Using negative selection, the galK cassette was exchanged using a template lacking aa 1156–1166 resulting in *nrg_ΔFERM*. All steps were performed according to the protocol provided by the NCI Frederick National Laboratory (http://ncifrederick.cancer.gov/research/brb/recombineeringInformation.aspx). All cloning steps were verified by sequencing. All constructs were inserted into the attP40 landing site using site-specific integration via the phi-C31 system (Bischof et al., 2007). All primers used in this study are listed in Table 1.

Cell culture, transfection, and cell aggregation assay

Schneider's line 2 (S2) cells were maintained in complete Schneider's medium at 25°C with air as the gas phase. Cells were transfected using X-tremeGENE HP DNA Transfection Reagent (Roche). Expression of transfected constructs was allowed for 3 d. Differently transfected cell populations were mixed in 2 ml Cryo tubes (Eppendorf) and incubated on a nutator for 2 h to allow for cell aggregation. For imaging, cells were pipetted onto microscope slides and images were captured using a laser scanning confocal microscope (TSC-SPE; Leica). For quantification, six

images were captured at fixed positions and quantified manually using ImageJ software.

Western blot analysis

Larval brains from wandering third instar larvae were dissected and transferred into 2× sample buffer (Life Technologies). NuPage gels (Invitrogen) were loaded with five brains per lane. Western blotting was performed according to Enneking et al. (2013). In brief, membranes were incubated overnight at 4°C with the following primary antibodies: mouse anti-Nrg^{3C1}, which recognizes extracellular domains of Nrg^{180} and Nrg^{167} (1:500; a gift from M. Hortsch, University of Michigan, Ann Arbor, MI; Hortsch et al., 1990); mouse anti-Nrg^{180} (BP104; 1:200; Hortsch et al., 1990); and mouse anti–β-tubulin (E7; 1:50; both from the Developmental Studies Hybridoma Bank) followed by a 2-h incubation at room temperature with secondary HRP-conjugated goat anti–mouse and goat anti–rabbit at 1:10,000 (Jackson ImmunoResearch Laboratories, Inc.).

Online supplemental material

Fig. S1 compares the wild-type MB architecture to the phenotype of nrg^{849} and nrg^{14}; P[nrg^{180}_ΔC] mutants at the end of larval development. Fig. S2 shows the axon midline crossing phenotype of αβ core neurons in nrg^{14}; P[nrg^{180}_YF] mutant animals. Fig. S3 demonstrates the cell adhesive functions of wild-type and mutant Nrg protein using an S2 cell aggregation assay. Fig. S4 summarizes the cell type–specific requirements of the different Nrg domains. Online supplemental material is available at http://www.jcb.org/cgi/content/full/jcb.201407131/DC1.

We would like to thank L. Luo and T. Lee, as well as the Bloomington Stock Center, the Drosophila Genomics Research Center, the Kyoto Stock Center, the Vienna Drosophila RNAi Center, and the Developmental Studies Hybridoma Bank for fly stocks, cDNAs, and antibodies. We thank the FMI sequencing and imaging facility and all members of the Pielage laboratory for helpful discussions.

Research in the laboratory of J. Pielage was supported by the Swiss National Science Foundation and the Friedrich Miescher Foundation.

The authors declare no competing financial interests.

Author contributions: D. Siegenthaler performed all experiments. E.M. Enneking generated constructs and fly stocks. E. Moreno generated constructs. D. Siegenthaler and J. Pielage designed experiments, analyzed data, and wrote the manuscript.

Submitted: 28 July 2014
Accepted: 24 February 2015

References

Adams, M.D., S.E. Celniker, R.A. Holt, C.A. Evans, J.D. Gocayne, P.G. Amanatides, S.E. Scherer, P.W. Li, R.A. Hoskins, R.F. Galle, et al. 2000. The genome sequence of *Drosophila melanogaster*. *Science*. 287:2185–2195. http://dx.doi.org/10.1126/science.287.5461.2185

Aso, Y., K. Grübel, S. Busch, A.B. Friedrich, I. Siwanowicz, and H. Tanimoto. 2009. The mushroom body of adult *Drosophila* characterized by GAL4 drivers. *J. Neurogenet.* 23:156–172. http://dx.doi.org/10.1080/01677060802471718

Bates, K.E., C.S. Sung, and S. Robinow. 2010. The unfulfilled gene is required for the development of mushroom body neuropil in *Drosophila*. *Neural Dev.* 5:4. http://dx.doi.org/10.1186/1749-8104-5-4

Bieber, A.J., P.M. Snow, M. Hortsch, N.H. Patel, J.R. Jacobs, Z.R. Traquina, J. Schilling, and C.S. Goodman. 1989. *Drosophila* neuroglian: a member of the immunoglobulin superfamily with extensive homology to the vertebrate neural adhesion molecule L1. *Cell*. 59:447–460. http://dx.doi.org/10.1016/0092-8674(89)90029-9

Bischof, J., R.K. Maeda, M. Hediger, F. Karch, and K. Basler. 2007. An optimized transgenesis system for *Drosophila* using germ-line-specific phiC31 integrases. *Proc. Natl. Acad. Sci. USA*. 104:3312–3317. http://dx.doi.org/10.1073/pnas.0611511104

Blum, A.L., W. Li, M. Cressy, and J. Dubnau. 2009. Short- and long-term memory in *Drosophila* require cAMP signaling in distinct neuron types. *Curr. Biol.* 19:1341–1350. http://dx.doi.org/10.1016/j.cub.2009.07.016

Boyle, M., A. Nighorn, and J.B. Thomas. 2006. *Drosophila* Eph receptor guides specific axon branches of mushroom body neurons. *Development*. 133:1845–1854. http://dx.doi.org/10.1242/dev.02353

Carhan, A., F. Allen, J.D. Armstrong, M. Hortsch, S.F. Goodwin, and K.M. O'Dell. 2005. Female receptivity phenotype of icebox mutants caused by a mutation in the L1-type cell adhesion molecule neuroglian. *Genes Brain Behav.* 4:449–465. (published erratum appears in *Genes Brain Behav.* 5:432) http://dx.doi.org/10.1111/j.1601-183X.2004.00117.x

Castellani, V., E. De Angelis, S. Kenwrick, and G. Rougon. 2002. Cis and trans interactions of L1 with neuropilin-1 control axonal responses to semaphorin 3A. *EMBO J.* 21:6348–6357. http://dx.doi.org/10.1093/emboj/cdf645

Chen, Y., D. Magnani, T. Theil, T. Pratt, and D.J. Price. 2012. Evidence that descending cortical axons are essential for thalamocortical axons to cross the pallial-subpallial boundary in the embryonic forebrain. *PLoS ONE*. 7:e33105. http://dx.doi.org/10.1371/journal.pone.0033105

Cheng, L., K. Itoh, and V. Lemmon. 2005. L1-mediated branching is regulated by two ezrin-radixin-moesin (ERM)-binding sites, the RSLE region and a novel juxtamembrane ERM-binding region. *J. Neurosci.* 25:395–403. http://dx.doi.org/10.1523/JNEUROSCI.4097-04.2005

Crittenden, J.R., E.M. Skoulakis, K.A. Han, D. Kalderon, and R.L. Davis. 1998. Tripartite mushroom body architecture revealed by antigenic markers. *Learn. Mem.* 5:38–51.

Davis, J.Q., and V. Bennett. 1994. Ankyrin binding activity shared by the neurofascin/L1/NrCAM family of nervous system cell adhesion molecules. *J. Biol. Chem.* 269:27163–27166.

de Belle, J.S., and M. Heisenberg. 1994. Associative odor learning in *Drosophila* abolished by chemical ablation of mushroom bodies. *Science*. 263:692–695. http://dx.doi.org/10.1126/science.8303280

Dickson, T.C., C.D. Mintz, D.L. Benson, and S.R. Salton. 2002. Functional binding interaction identified between the axonal CAM L1 and members of the ERM family. *J. Cell Biol.* 157:1105–1112. http://dx.doi.org/10.1083/jcb.200111076

Dubreuil, R.R., G. MacVicar, S. Dissanayake, C. Liu, D. Homer, and M. Hortsch. 1996. Neuroglian-mediated cell adhesion induces assembly of the membrane skeleton at cell contact sites. *J. Cell Biol.* 133:647–655. http://dx.doi.org/10.1083/jcb.133.3.647

Enneking, E.M., S.R. Kudumala, E. Moreno, R. Stephan, J. Boerner, T.A. Godenschwege, and J. Pielage. 2013. Transsynaptic coordination of synaptic growth, function, and stability by the L1-type CAM Neuroglian. *PLoS Biol.* 11:e1001537. http://dx.doi.org/10.1371/journal.pbio.1001537

Fransen, E., V. Lemmon, G. Van Camp, L. Vits, P. Coucke, and P.J. Willems. 1995. CRASH syndrome: clinical spectrum of corpus callosum hypoplasia, retardation, adducted thumbs, spastic paraparesis and hydrocephalus due to mutations in one single gene, L1. *Eur. J. Hum. Genet.* 3:273–284.

Fransen, E., G. Van Camp, R. D'Hooge, L. Vits, and P.J. Willems. 1998. Genotype-phenotype correlation in L1 associated diseases. *J. Med. Genet.* 35:399–404. http://dx.doi.org/10.1136/jmg.35.5.399

Fushima, K., and H. Tsujimura. 2007. Precise control of fasciclin II expression is required for adult mushroom body development in *Drosophila*. *Dev. Growth Differ.* 49:215–227. http://dx.doi.org/10.1111/j.1440-169X.2007.00922.x

Gallarda, B.W., D. Bonanomi, D. Müller, A. Brown, W.A. Alaynick, S.E. Andrews, G. Lemke, S.L. Pfaff, and T. Marquardt. 2008. Segregation of axial motor and sensory pathways via heterotypic trans-axonal signaling. *Science*. 320:233–236. http://dx.doi.org/10.1126/science.1153758

García-Alonso, L., S. Romani, and F. Jiménez. 2000. The EGF and FGF receptors mediate neuroglian function to control growth cone decisions during sensory axon guidance in *Drosophila*. *Neuron*. 28:741–752. http://dx.doi.org/10.1016/S0896-6273(00)00150-1

Gardiol, A., and D. St Johnston. 2014. Staufen targets coracle mRNA to *Drosophila* neuromuscular junctions and regulates GluRIIA synaptic accumulation and bouton number. *Dev. Biol.* 392:153–167. http://dx.doi.org/10.1016/j.ydbio.2014.06.007

Garver, T.D., Q. Ren, S. Tuvia, and V. Bennett. 1997. Tyrosine phosphorylation at a site highly conserved in the L1 family of cell adhesion molecules abolishes ankyrin binding and increases lateral mobility of neurofascin. *J. Cell Biol.* 137:703–714. http://dx.doi.org/10.1083/jcb.137.3.703

Genova, J.L., and R.G. Fehon. 2003. Neuroglian, Gliotactin, and the Na^+/K^+ ATPase are essential for septate junction function in *Drosophila*. *J. Cell Biol.* 161:979–989. http://dx.doi.org/10.1083/jcb.200212054

Gil, O.D., T. Sakurai, A.E. Bradley, M.Y. Fink, M.R. Cassella, J.A. Kuo, and D.P. Felsenfeld. 2003. Ankyrin binding mediates L1CAM interactions with static components of the cytoskeleton and inhibits retrograde movement of L1CAM on the cell surface. *J. Cell Biol.* 162:719–730. http://dx.doi.org/10.1083/jcb.200211011

Goossens, T., Y.Y. Kang, G. Wuytens, P. Zimmermann, Z. Callaerts-Végh, G. Pollarolo, R. Islam, M. Hortsch, and P. Callaerts. 2011. The *Drosophila* L1CAM homolog Neuroglian signals through distinct pathways to control different aspects of mushroom body axon development. *Development*. 138:1595–1605. http://dx.doi.org/10.1242/dev.052787

Gordon, M.D., and K. Scott. 2009. Motor control in a *Drosophila* taste circuit. *Neuron*. 61:373–384. http://dx.doi.org/10.1016/j.neuron.2008.12.033

Grillenzoni, N., A. Flandre, C. Lasbleiz, and J.M. Dura. 2007. Respective roles of the DRL receptor and its ligand WNT5 in *Drosophila* mushroom body development. *Development*. 134:3089–3097. http://dx.doi.org/10.1242/dev.02876

Hall, S.G., and A.J. Bieber. 1997. Mutations in the *Drosophila* neuroglian cell adhesion molecule affect motor neuron pathfinding and peripheral nervous system patterning. *J. Neurobiol.* 32:325–340. http://dx.doi.org/10.1002/(SICI)1097-4695(199703)32:3<325::AID-NEU6>3.0.CO;2-9

Heisenberg, M. 2003. Mushroom body memoir: from maps to models. *Nat. Rev. Neurosci.* 4:266–275. http://dx.doi.org/10.1038/nrn1074

Hortsch, M. 2000. Structural and functional evolution of the L1 family: are four adhesion molecules better than one? *Mol. Cell. Neurosci.* 15:1–10. http://dx.doi.org/10.1006/mcne.1999.0809

Hortsch, M., A.J. Bieber, N.H. Patel, and C.S. Goodman. 1990. Differential splicing generates a nervous system-specific form of *Drosophila* neuroglian. *Neuron*. 4:697–709. http://dx.doi.org/10.1016/0896-6273(90)90196-M

Hortsch, M., Y.M. Wang, Y. Marikar, and A.J. Bieber. 1995. The cytoplasmic domain of the *Drosophila* cell adhesion molecule neuroglian is not essential for its homophilic adhesive properties in S2 cells. *J. Biol. Chem.* 270:18809–18817. http://dx.doi.org/10.1074/jbc.270.32.18809

Hortsch, M., D. Homer, J.D. Malhotra, S. Chang, J. Frankel, G. Jefford, and R.R. Dubreuil. 1998. Structural requirements for outside-in and inside-out signaling by *Drosophila* neuroglian, a member of the L1 family of cell adhesion molecules. *J. Cell Biol.* 142:251–261. http://dx.doi.org/10.1083/jcb.142.1.251

Jouet, M., A. Rosenthal, G. Armstrong, J. MacFarlane, R. Stevenson, J. Paterson, A. Metzenberg, V. Ionasescu, K. Temple, and S. Kenwrick. 1994. X-linked spastic paraplegia (SPG1), MASA syndrome and X-linked hydrocephalus result from mutations in the L1 gene. *Nat. Genet.* 7:402–407. http://dx.doi.org/10.1038/ng0794-402

Kamiguchi, H., M.L. Hlavin, M. Yamasaki, and V. Lemmon. 1998. Adhesion molecules and inherited diseases of the human nervous system. *Annu. Rev. Neurosci.* 21:97–125. http://dx.doi.org/10.1146/annurev.neuro.21.1.97

Koester, S.E., and D.D. O'Leary. 1994. Axons of early generated neurons in cingulate cortex pioneer the corpus callosum. *J. Neurosci.* 14:6608–6620.

Kolodkin, A.L., and M. Tessier-Lavigne. 2011. Mechanisms and molecules of neuronal wiring: a primer. *Cold Spring Harb. Perspect. Biol.* 3:a001727. http://dx.doi.org/10.1101/cshperspect.a001727

Krashes, M.J., A.C. Keene, B. Leung, J.D. Armstrong, and S. Waddell. 2007. Sequential use of mushroom body neuron subsets during *Drosophila* odor memory processing. *Neuron*. 53:103–115. http://dx.doi.org/10.1016/j.neuron.2006.11.021

Kurusu, M., T. Awasaki, L.M. Masuda-Nakagawa, H. Kawauchi, K. Ito, and K. Furukubo-Tokunaga. 2002. Embryonic and larval development of the *Drosophila* mushroom bodies: concentric layer subdivisions and the role of fasciclin II. *Development*. 129:409–419.

Lee, T., and L. Luo. 1999. Mosaic analysis with a repressible cell marker for studies of gene function in neuronal morphogenesis. *Neuron*. 22:451–461. http://dx.doi.org/10.1016/S0896-6273(00)80701-1

Lee, T., A. Lee, and L. Luo. 1999. Development of the *Drosophila* mushroom bodies: sequential generation of three distinct types of neurons from a neuroblast. *Development*. 126:4065–4076.

Lyuksyutova, A.I., C.C. Lu, N. Milanesio, L.A. King, N. Guo, Y. Wang, J. Nathans, M. Tessier-Lavigne, and Y. Zou. 2003. Anterior-posterior guidance of commissural axons by Wnt-frizzled signaling. *Science*. 302:1984–1988. http://dx.doi.org/10.1126/science.1089610

Maness, P.F., and M. Schachner. 2007. Neural recognition molecules of the immunoglobulin superfamily: signaling transducers of axon guidance and neuronal migration. *Nat. Neurosci.* 10:19–26. http://dx.doi.org/10.1038/nn1827

McCartney, B.M., and R.G. Fehon. 1996. Distinct cellular and subcellular patterns of expression imply distinct functions for the Drosophila homologues of moesin and the neurofibromatosis 2 tumor suppressor, merlin. *J. Cell Biol.* 133:843–852. http://dx.doi.org/10.1083/jcb.133.4.843

Ng, J., T. Nardine, M. Harms, J. Tzu, A. Goldstein, Y. Sun, G. Dietzl, B.J. Dickson, and L. Luo. 2002. Rac GTPases control axon growth, guidance and branching. *Nature*. 416:442–447. http://dx.doi.org/10.1038/416442a

Nishikimi, M., K. Oishi, and K. Nakajima. 2013. Axon guidance mechanisms for establishment of callosal connections. *Neural Plast.* 2013:149060.

Pielage, J., L. Cheng, R.D. Fetter, P.M. Carlton, J.W. Sedat, and G.W. Davis. 2008. A presynaptic giant ankyrin stabilizes the NMJ through regulation of presynaptic microtubules and transsynaptic cell adhesion. *Neuron*. 58:195–209. http://dx.doi.org/10.1016/j.neuron.2008.02.017

Pielage, J., V. Bulat, J.B. Zuchero, R.D. Fetter, and G.W. Davis. 2011. Hts/Adducin controls synaptic elaboration and elimination. *Neuron*. 69:1114–1131. http://dx.doi.org/10.1016/j.neuron.2011.02.007

Qin, H., M. Cressy, W. Li, J.S. Coravos, S.A. Izzi, and J. Dubnau. 2012. Gamma neurons mediate dopaminergic input during aversive olfactory memory formation in Drosophila. *Curr. Biol.* 22:608–614. http://dx.doi.org/10.1016/j.cub.2012.02.014

Ramel, D., X. Wang, C. Laflamme, D.J. Montell, and G. Emery. 2013. Rab11 regulates cell-cell communication during collective cell movements. *Nat. Cell Biol.* 15:317–324. http://dx.doi.org/10.1038/ncb2681

Sakurai, T. 2012. The role of NrCAM in neural development and disorders—beyond a simple glue in the brain. *Mol. Cell. Neurosci.* 49:351–363. http://dx.doi.org/10.1016/j.mcn.2011.12.002

Sakurai, T., O.D. Gil, J.D. Whittard, M. Gazdoiu, T. Joseph, J. Wu, A. Waksman, D.L. Benson, S.R. Salton, and D.P. Felsenfeld. 2008. Interactions between the L1 cell adhesion molecule and ezrin support traction-force generation and can be regulated by tyrosine phosphorylation. *J. Neurosci. Res.* 86:2602–2614. http://dx.doi.org/10.1002/jnr.21705

Schmidt, E.R., S. Brignani, Y. Adolfs, S. Lemstra, J. Demmers, M. Vidaki, A.L. Donahoo, K. Lilleväli, E. Vasar, L.J. Richards, et al. 2014. Subdomain-mediated axon-axon signaling and chemoattraction cooperate to regulate afferent innervation of the lateral habenula. *Neuron*. 83:372–387. http://dx.doi.org/10.1016/j.neuron.2014.05.036

Schwabe, T., J.A. Borycz, I.A. Meinertzhagen, and T.R. Clandinin. 2014. Differential adhesion determines the organization of synaptic fascicles in the *Drosophila* visual system. *Curr. Biol.* 24:1304–1313. http://dx.doi.org/10.1016/j.cub.2014.04.047

Shin, J.E., and A. DiAntonio. 2011. Highwire regulates guidance of sister axons in the *Drosophila* mushroom body. *J. Neurosci.* 31:17689–17700. http://dx.doi.org/10.1523/JNEUROSCI.3902-11.2011

Strauss, R., and M. Heisenberg. 1993. A higher control center of locomotor behavior in the *Drosophila* brain. *J. Neurosci.* 13:1852–1861.

Suter, D.M., L.D. Errante, V. Belotserkovsky, and P. Forscher. 1998. The Ig superfamily cell adhesion molecule, apCAM, mediates growth cone steering by substrate-cytoskeletal coupling. *J. Cell Biol.* 141:227–240. http://dx.doi.org/10.1083/jcb.141.1.227

Tanaka, N.K., H. Tanimoto, and K. Ito. 2008. Neuronal assemblies of the *Drosophila* mushroom body. *J. Comp. Neurol.* 508:711–755. http://dx.doi.org/10.1002/cne.21692

Tovar-Moll, F., J. Moll, R. de Oliveira-Souza, I. Bramati, P.A. Andreiuolo, and R. Lent. 2007. Neuroplasticity in human callosal dysgenesis: a diffusion tensor imaging study. *Cereb. Cortex*. 17:531–541. http://dx.doi.org/10.1093/cercor/bhj178

Trannoy, S., C. Redt-Clouet, J.M. Dura, and T. Preat. 2011. Parallel processing of appetitive short- and long-term memories in *Drosophila*. *Curr. Biol.* 21:1647–1653. http://dx.doi.org/10.1016/j.cub.2011.08.032

Tuvia, S., T.D. Garver, and V. Bennett. 1997. The phosphorylation state of the FIGQY tyrosine of neurofascin determines ankyrin-binding activity and patterns of cell segregation. *Proc. Natl. Acad. Sci. USA*. 94:12957–12962. http://dx.doi.org/10.1073/pnas.94.24.12957

Venken, K.J., J.W. Carlson, K.L. Schulze, H. Pan, Y. He, R. Spokony, K.H. Wan, M. Koriabine, P.J. de Jong, K.P. White, et al. 2009. Versatile P[acman] BAC libraries for transgenesis studies in *Drosophila melanogaster*. *Nat. Methods*. 6:431–434. http://dx.doi.org/10.1038/nmeth.1331

Vits, L., G. Van Camp, P. Coucke, E. Fransen, K. De Boulle, E. Reyniers, B. Korn, A. Poustka, G. Wilson, C. Schrander-Stumpel, et al. 1994. MASA syndrome is due to mutations in the neural cell adhesion gene L1CAM. *Nat. Genet.* 7:408–413. http://dx.doi.org/10.1038/ng0794-408

Wang, J., C.T. Zugates, I.H. Liang, C.H. Lee, and T. Lee. 2002. *Drosophila* Dscam is required for divergent segregation of sister branches and suppresses ectopic bifurcation of axons. *Neuron*. 33:559–571. http://dx.doi.org/10.1016/S0896-6273(02)00570-6

Wong, E.V., S. Kenwrick, P. Willems, and V. Lemmon. 1995. Mutations in the cell adhesion molecule L1 cause mental retardation. *Trends Neurosci.* 18:168–172. http://dx.doi.org/10.1016/0166-2236(95)93896-6

Wu, C.L., M.F. Shih, P.T. Lee, and A.S. Chiang. 2013. An octopamine-mushroom body circuit modulates the formation of anesthesia-resistant memory in *Drosophila*. *Curr. Biol.* 23:2346–2354. http://dx.doi.org/10.1016/j.cub.2013.09.056

Yamasaki, M., P. Thompson, and V. Lemmon. 1997. CRASH syndrome: mutations in L1CAM correlate with severity of the disease. *Neuropediatrics*. 28:175–178. http://dx.doi.org/10.1055/s-2007-973696

Yoshikawa, S., R.D. McKinnon, M. Kokel, and J.B. Thomas. 2003. Wnt-mediated axon guidance via the *Drosophila* Derailed receptor. *Nature*. 422:583–588. http://dx.doi.org/10.1038/nature01522

Zhan, X.L., J.C. Clemens, G. Neves, D. Hattori, J.J. Flanagan, T. Hummel, M.L. Vasconcelos, A. Chess, and S.L. Zipursky. 2004. Analysis of Dscam diversity in regulating axon guidance in *Drosophila* mushroom bodies. *Neuron*. 43:673–686. http://dx.doi.org/10.1016/j.neuron.2004.07.020